African Journal of Mathematics and Statistics Studies
ISSN: 2689-5323
Volume 8, Issue 3, 2025 (pp. 136-161)
www.abjournals.org

TRANSMISSION DYNAMICS AND CONTROL OF A DETERMINISTIC BIRD-HUMAN AVIAN INFLUENZA MODEL

J. A. Akingbade[1*] and O. M. Bamigbola[2]

[1,2]Department of Mathematics, Faculty of Physical Sciences, University of Ilorin, Ilorin, Kwara State, Nigeria.

[*]Corresponding Author's Email: jaakingbade@yahoo.com

Cite this article:

J. A. Akingbade, O. M. Bamigbola (2025), Transmission Dynamics and Control of a Deterministic Bird-Human Avian Influenza Model. African Journal of Mathematics and Statistics Studies 8(3), 136-161. DOI: 10.52589/AJMSS-KSUGFI1Z

Manuscript History

Received: 7 Jun 2025

Accepted: 9 Jul 2025

Published: 14 Aug 2025

ABSTRACT: *This paper develops a deterministic model to analyze the transmission dynamics and control measures of avian influenza, with a specific emphasis on bird-to-human transmission. The model innovatively integrates key intervention measures, including vaccination, treatment, and quarantine, while categorizing the human population into seven distinct classes and the bird population into four. A dynamic analysis is conducted to elucidate the epidemiological characteristics and potential control measures for avian influenza outbreaks. The qualitative properties of the model are rigorously assessed using the Jacobian matrix, and the basic reproductive ratios are calculated utilizing the next-generation matrix approach. A stability analysis of the equilibrium states is performed through the trace and determinant of the Jacobian matrix, revealing the existence of two key equilibria: the disease-free equilibrium and an endemic equilibrium. Simulation experiments show that the synergistic application of all three control measures significantly reduces infection rates compared to the implementation of individual or paired strategies. Furthermore, a sensitivity analysis highlights the most influential parameters affecting control outcomes, enhancing the understanding of effective management strategies. This research provides valuable insights into managing avian influenza transmission, contributing to the broader discourse on infectious disease control in avian and human populations.*

2020 Mathematics Subject Classification: 34A34, 34C60, 34D20, 34D23, Secondary 92B05, 92C60.

KEYWORDS: Avian influenza; deterministic model; basic reproductive number; sensitivity analysis; epidemiological modelling.

Article DOI: 10.52589/AJMSS-KSUGFI1Z
DOI URL: https://doi.org/10.52589/AJMSS-KSUGFI1Z

African Journal of Mathematics and Statistics Studies
ISSN: 2689-5323
Volume 8, Issue 3, 2025 (pp. 136-161)

www.abjournals.org

INTRODUCTION

Avian influenza, commonly referred to as bird flu, is a severe and highly contagious viral infection that predominantly targets the respiratory system. The disease has seasonal outbreaks each year, leading to significant illness and causing the deaths of hundreds of thousands of individuals globally. Modnak [26] and David et al. [14] classify influenza A viruses that infect birds into two categories: Low Pathogenic Avian Influenza (LPAI) and High Pathogenic Avian Influenza (HPAI). There are four types of influenza viruses: A, B, C, and D. Types A and B are responsible for seasonal flu outbreaks in humans, type C is uncommon and usually causes mild respiratory symptoms without leading to epidemics, and type D primarily affects cattle. Between 21 September and 6 December 2024, 657 highly pathogenic avian influenza (HPAI) A(H5N1) and A(H5N5) virus detections were reported in domestic (341) and wild (316) birds across 27 countries in Europe [7].

Avian influenza is highly severe, with a mortality rate of about 60%, resulting in numerous hospitalizations, deaths, and significant economic impacts. Infected birds usually show symptoms within two to seven days, depending on the virus strain [14, 26]. A 2012 publication by the Centers for Disease Control and Prevention (CDCP) [11, 12] states that influenza in humans can range from mild to severe illness and, in some cases, can be fatal. Common symptoms of the flu include fever or chills, cough, sore throat, runny or stuffy nose, muscle or body aches, headaches, fatigue, and shortness of breath. Between 21 September and 11 December 2024, 56 new human cases of avian influenza virus infection were reported from North America (45 A(H5N1) cases), Viet Nam (one A(H5)) and China (10 A(H9N2) cases). Most of North America's A(H5) human cases ($95.6\%, n = 43/45$) had reported exposure to poultry, live poultry markets, or dairy cattle before avian influenza virus detection or onset of illness [7].According to Gubar and Quanyan [18], prevention or suppression of avian influenza in infected patients can be achieved through non-pharmaceutical interventions, such as isolation and quarantine, as well as pharmaceutical measures, including the use of antivirals and vaccines. The most effective prevention strategy is to avoid exposure to sources of the flu. Since different types of bird flu can cause varying symptoms, treatment approaches may differ accordingly. As a highly communicable disease, avian influenza presents significant challenges to both bird and human populations globally. Therefore, implementing control and prevention strategies is essential to combat the threat posed by avian influenza infections. Over the past two decades, numerous epidemiological models have been developed based on the classical Susceptible-Infected-Removed (SIR) framework to predict the spread of influenza.

Evirgen $et\ al.$ [16] introduced a novel model for influenza A dynamics utilizing the Caputo-Fabrizio fractional derivative operator, focusing on distinct contact rates between exposed and infected individuals. They established the existence and uniqueness of the solution, derived a series solution for all compartments via the Laplace transform method, and analyzed the reproduction number to assess contact rate effectiveness. By applying the predictor-corrector method, they demonstrated the effectiveness of the fractional derivative in accurately predicting disease dynamics, highlighting its potential to improve disease modeling and enhance understanding of influenza A mechanisms.

Tingting $et\ al.$ [34] developed a time-periodic reaction-diffusion model to analyze avian influenza virus transmission among birds, poultry, and humans, incorporating environmental

Article DOI: 10.52589/AJMSS-KSUGFI1Z
DOI URL: https://doi.org/10.52589/AJMSS-KSUGFI1Z

African Journal of Mathematics and Statistics Studies
ISSN: 2689-5323
Volume 8, Issue 3, 2025 (pp. 136-161)

www.abjournals.org

transmission and spatial heterogeneity. Their study confirmed the well-posedness of solutions and characterized the basic reproduction number R_0 as a threshold for global dynamics. They demonstrated the existence of an endemic equilibrium and its global attractiveness in the autonomous model. Additionally, numerical simulations illustrated the theoretical results and assessed the impact of various parameters on R_0.

Hayama $et\ al.$ [19] assert the critical importance of early detection in effectively controlling outbreaks of highly pathogenic avian influenza (HPAI) on poultry farms. Through a thorough analysis of daily mortality data from twelve broiler chicken farms during the 2020-2021 H5N8 outbreak in Japan, the authors applied a Susceptible-Exposed-Infectious-Removed (SEIR) model to rigorously assess transmission dynamics. Their results reveal a median transmission rate of 1.449 per day, with a significant time window of 14.0 days from the introduction of the virus to the notification. Furthermore, the stochastic model demonstrates that this window can extend to 21 days, with a range of 12 to 34 days. Importantly, the study identifies that older birds correspond to lower transmission rates and longer notification delays (p-value = 0.02). This research unequivocally provides essential insights that will enhance early detection efforts and strengthen tracing protocols for managing avian influenza outbreaks effectively. In the paper by Imran [20], a deterministic model is developed to explore the transmission dynamics of influenza, highlighting the significance of hospitalization effects and diffusion. The model is represented as a system of partial differential equations, solved using some numerical techniques. The study also calculates the basic reproduction number, ensuring local stability of a disease-free equilibrium in the absence of diffusion. Additionally, various numerical simulations illustrate how different input parameter values influence the steady-state conditions across the population compartments, particularly emphasizing the impact of the effective contact rate.

Putri and Syafwan [28] explore the application of mathematical modeling as a strategic tool for controlling epidemics in their study. They develop a foundational model to analyze the bird flu epidemic, emphasizing vaccination as a key method for disease management. The authors reformulate their bird flu model to account for the effects of vaccination, representing the system using ordinary differential equations. Their work also includes a discussion on the stability of both models, linking stability to a threshold number that determines whether a population remains free of the bird flu virus or becomes infected. To validate their analytical findings, the authors present numerical solutions illustrated on a phase plane. Alexander $et\ al.$ [8] developed a mathematical model to explore the transmission dynamics of influenza and evaluate the impact of immunization using a partially effective vaccine. The model includes the recruitment of infected individuals, which is identified as a critical factor in understanding the transmission dynamics of the disease. Their analysis considers two scenarios: one where the population does not admit new infected individuals and another where there is an inflow of infective individuals. The model incorporates vaccination with a known efficacy, highlighting the importance of immunization in controlling the spread of influenza within the population.

Tchuenche et al. [30] developed and analyzed an influenza pandemic model incorporating vaccination and treatment, considering two preventive scenarios with varying vaccine uptake: increasing and decreasing. The model uses a Susceptible-Vaccinated-Infected-Treatment-Recovered $(S-V-I-T-R)$ framework to capture the dynamics of the pandemic. Given the need for a deeper understanding of the history, transmission, and control strategies

Article DOI: 10.52589/AJMSS-KSUGFI1Z
DOI URL: https://doi.org/10.52589/AJMSS-KSUGFI1Z

of avian influenza, this paper expands the classification of avian influenza infection to include a broader range of classes. The study employs both analytical and numerical methods to address the transmission dynamics and control of the flu from birds to humans using a deterministic model. This model extends the traditional Susceptible-Infected-Recovered $(S-I-R)$ framework in an open population [5, 6, 22] to include the following additional compartments: Susceptible birds (S_b), Vaccinated birds (V_b), Exposed birds (E_b), Infected birds (I_b), Susceptible humans (S_h), Vaccinated humans (V_h), Exposed humans (E_h), Infected humans (I_h), Quarantined individuals (Q), Treated individuals (T), and Recovered individuals (R). The paper then discusses the qualitative properties of the solution and presents numerical simulations to support the findings.

MATHEMATICAL FORMULATION OF THE MODEL

Assumptions of Avian influenza Model

The model formulation is based on the following assumptions:

- Infection occurs due to human contact with infected birds.
- Entry into both the bird and human population is open, and the way of exit is through mortality from natural causes or death caused by infection.
- A proportion of the recruited individuals are either immunized or not against avian influenza.
- Vaccination of both susceptible birds and humans is done at the initial stage.
- The people with active immunity in the susceptible compartment moved directly to the recovered compartment without being infected.
- The avian influenza disease is assumed to confer temporary immunity. Therefore, individuals in this category recovered and became susceptible again.
- The people in each compartment have an equal mortality or natural death rate μ.

Model Description

In this section, a mathematical model is formulated to describe the dynamics and transmission of avian influenza from birds to the human population. The model is both compartmental and deterministic, encompassing compartments for birds $(S_b - V_b - E_b - I_b)$ and humans $(S_h - V_h - E_h - I_h - Q - T - R)$. It incorporates epidemiological features that capture the infection dynamics between birds and humans in an open population using a system of ordinary differential equations and bilinear incidence.

The model builds on the basic Susceptible-Infected-Recovered $(S-I-R)$ framework from Kermack but extends it to an open population by including recruitment into both human and bird populations, with additional compartments for vaccination, exposure, quarantine, and treatment.

Article DOI: 10.52589/AJMSS-KSUGFI1Z
DOI URL: https://doi.org/10.52589/AJMSS-KSUGFI1Z

African Journal of Mathematics and Statistics Studies
ISSN: 2689-5323
Volume 8, Issue 3, 2025 (pp. 136-161)
www.abjournals.org

The total population of both humans and birds at any time t is represented by $N_h(t)$ and $N_b(t)$ given as $N_h(t) = S_h + V_h + E_h + I_h + Q + T + R$ and $N_b(t) = S_b + V_b + E_b + I_b$. It is important to note that when an individual comes into contact with an infected bird or consumes uncooked parts of an infected bird, the virus begins to multiply within the cells. Considering the above factors, the schematic flow diagram for the avian influenza model is presented in Figure 1.

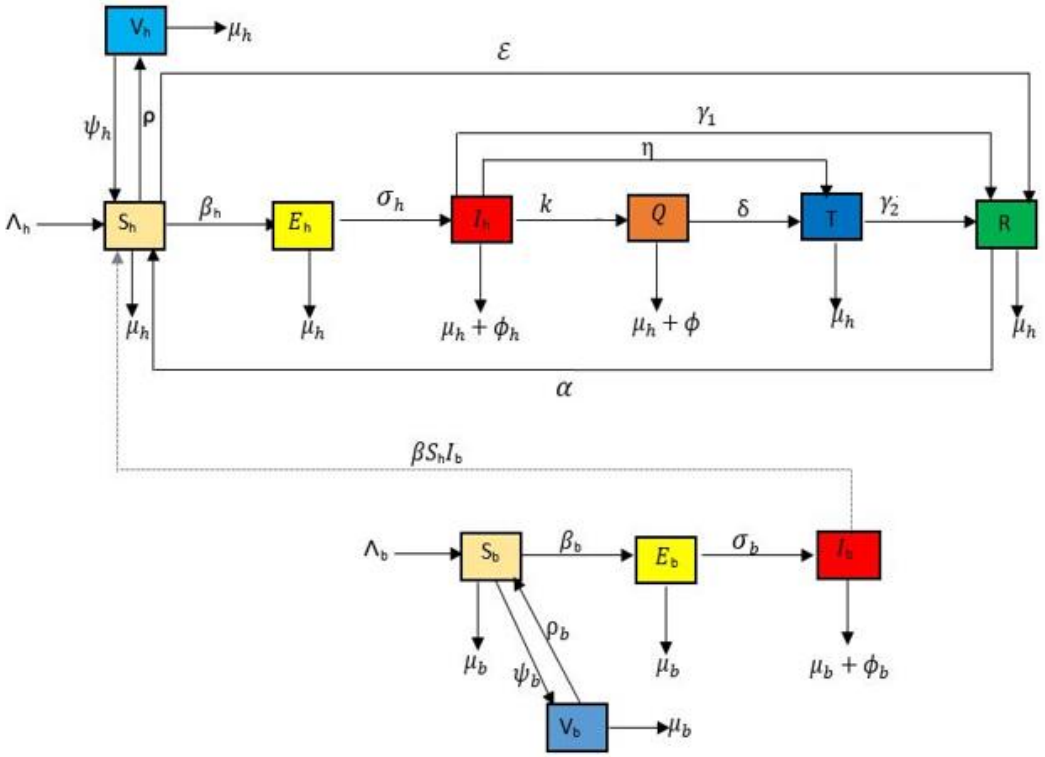

Figure 1: Flowchart of avian influenza transmission model with intervention

Table 1: Parameters of the avian influenza model

Symbol	Description
Λ_h	Human recruitment rate
Λ_b	Bird recruitment rate
β_h	Effective contact rate from human-to-human
β_b	Effective contact rate from bird-to-bird
β	Effective contact rate from bird-to human
ε	Immunity gain
σ_h	Progression rate from exposed human to infectious human class
σ_b	Progression rate from exposed bird to infectious bird class
γ_1	Rate at which infected human recovered naturally
γ_2	Recovery rate of human due to treatment
ϕ_h	Death rate of human due to avian influenza

Article DOI: 10.52589/AJMSS-KSUGFI1Z
DOI URL: https://doi.org/10.52589/AJMSS-KSUGFI1Z

African Journal of Mathematics and Statistics Studies
ISSN: 2689-5323
Volume 8, Issue 3, 2025 (pp. 136-161)
www.abjournals.org

ϕ_b	Death rate of birds due to avian influenza
ϕ	Death rate due to quarantine of infected humans
μ_h	Natural death/mortality rate of human from each class
μ_b	Natural death/mortality rate of birds from each class
α	Rate of immunity loss
ρ	The proportion of susceptible human to be vaccinated
ρ_b	The proportion of susceptible bird to be vaccinated
ψ_h	Rate at which human vaccine-based immunity wanes
ψ_b	Rate at which bird vaccine-based immunity wanes
k	Progression rate of human from infectious class to quarantine class
η	Rate at which infectious is being treated
δ	Quarantined human treatment rate

Model Equations

With the above assumptions depicted by the flowchart in Figure 1 and descriptions in Table 1, the following system of nonlinear ordinary differential equations describes the evolutionary dynamics of an avian influenza infection with a combination of interventions, and this is a new deterministic model:

$$\frac{dS_h}{dt} = \wedge_h - \beta S_h I_b - \beta_h S_h I_h - (\mu_h + \rho + \varepsilon)S_h + \alpha R + \psi_h V_h \ \frac{dV_h}{dt} = \rho S_h - (\psi_h + \mu_h)V_h \ \frac{dE_h}{dt} = \beta S_h I_b + \beta_h S_h I_h - (\mu_h + \sigma_h)E_h \ \frac{dI_h}{dt} = \sigma_h E_h - (k + \gamma_1 + \eta + \mu_h + \phi_h)I_h \ \frac{dQ}{dt} = kI_h - (\delta + \mu_h + \phi)Q \ \frac{dT}{dt} = \eta I_h + \delta Q - (\mu_h + \gamma_2 +)T \ \frac{dR}{dt} = \gamma_2 T + \gamma_1 I_h + \varepsilon S_h - (\mu_h + \alpha)R \ \frac{dS_b}{dt} = \wedge_b - \beta_b S_b I_b - (\mu_b + \rho_b)S_b + \psi_b V_b \ \frac{dV_b}{dt} = \rho_b S_b - (\psi_b + \mu_b)V_b \ \frac{dE_b}{dt} = \beta_b S_b I_b - (\sigma_b + \mu_b)E_b \ \frac{dI_b}{dt} = \sigma_b E_b - (\mu_b + \phi_b)I_b \ \} \quad (2.1)$$

with initial conditions $S_h(0) > 0, V_h(0) \geq 0, E_h(0) \geq 0, I_h(0) \geq 0, Q(0) \geq 0, T(0) \geq 0, R(0) \geq 0, S_b(0) > 0, V_b(0) \geq 0, E_b(0) \geq 0, I_b(0),$ where $N_h(t) = S_h + V_h + E_h + I_h + Q + T + R$ and $N_b(t) = S_b + V_b + E_b + I_b$

Feasibility Region and Positivity of Solutions of the Model

In this section, the basic properties of the model system (2.1) are employed to establish the criteria for positivity of solutions and well-posedness of the system.

Article DOI: 10.52589/AJMSS-KSUGFI1Z
DOI URL: https://doi.org/10.52589/AJMSS-KSUGFI1Z

African Journal of Mathematics and Statistics Studies
ISSN: 2689-5323
Volume 8, Issue 3, 2025 (pp. 136-161)
www.abjournals.org

Feasibility region of the model

The region in which the solution of model (2.1) lies is investigated because of its biological import.

Theorem 1. Let every solution, Ω, of model (2.1) with initial conditions in R_+^{11} (set of vectors with 11 non-negative components) for which changes in both humans and birds population hold, approach and stays in the domain of the solution as $t \to \infty$. Then, the feasible solution for the model is a positively invariant set given by $\Omega = \Omega_h \times \Omega_b = \left\{(S_h, V_h, E_h, I_h, Q, T, R, S_b, V_b, E_b, I_b) \in R_+^{11}: N_h(t) \leq \frac{\Lambda_h}{\mu_h}, N_b(t) \leq \frac{\Lambda_b}{\mu_b}\right\}$.

Proof. For human population in (2.1), changes of N_h leads to changes of all variables in the population (i.e., $N_h = S_h + V_h + E_h + I_h + Q + T + R$) we have

$$\frac{dN_h}{dt} = \frac{dS_h}{dt} + \frac{dV_h}{dt} + \frac{dE_h}{dt} + \frac{dI_h}{dt} + \frac{dQ}{dt} + \frac{dT}{dt} + \frac{dR}{dt} \tag{2.2}$$

$$\frac{dN_h}{dt} = \Lambda - \mu_h N_h(t) - \phi_h I_h - \phi Q, \tag{2.3}$$

In the absence of the disease ($\phi_h = \phi = 0$), (2.3) reduces to

$$\frac{dN_h}{dt} = \Lambda - \mu_h N_h(t). \tag{2.4}$$

Noting from Table 1 that ϕ_h and ϕ are non-negative real numbers leads to

$$\frac{dN_h}{dt} = \Lambda - \mu_h N_h(t) - \phi_h I_h - \phi Q \leq \Lambda - \mu_h N_h(t). \tag{2.5}$$

Thus,

$$\frac{dN_h}{dt} \leq \Lambda - \mu_h N_h(t), \tag{2.6}$$

which implies that

$$\frac{dN_h}{dt} + \mu_h N_h(t) \leq \Lambda_h. \tag{2.7}$$

Solving inequality (2.7) by the integrating factor approach yields

$$N_h(t) \leq N_h(0)e^{-\mu_h t} + \frac{\Lambda_h}{\mu}(1 - e^{-\mu_h t}). \tag{2.8}$$

Hence as $t \to \infty$, the population size, N_h, approaches $\frac{\Lambda_h}{\mu}$, which implies that $0 \leq N_h \leq \frac{\Lambda_h}{\mu_h}$, meaning that the trajectories of model (2.1) are bounded. Therefore, all feasible solutions of the human population of the model system (2.1) enter the region

$$\Omega_h = \left\{(S_h, V_h, E_h, I_h, Q, T, R) \in R_+^7: N_h(t) \leq \frac{\Lambda_h}{\mu_h}\right\}.$$

Article DOI: 10.52589/AJMSS-KSUGFI1Z
DOI URL: https://doi.org/10.52589/AJMSS-KSUGFI1Z

African Journal of Mathematics and Statistics Studies
ISSN: 2689-5323
Volume 8, Issue 3, 2025 (pp. 136-161)
www.abjournals.org

Similarly, for the birds population,

$$\frac{dN_b}{dt} = \frac{dS_b}{dt} + \frac{dV_b}{dt} + \frac{dE_b}{dt} + \frac{dI_b}{dt}. \qquad (2.9)$$

The case of the bird population in (2.1) is bounded as $0 \leq N_b \leq \frac{\Lambda_b}{\mu_b}$. Thus, the feasible solutions of the bird population also enters the region

$$\Omega_b = \left\{(S_b, V_b, E_b, I_b) \in R_+^4 : N_b(t) \leq \frac{\Lambda_b}{\mu_b}\right\},$$

Hence, the feasible solution set for the system (2.1) is given by

$$\Omega = \left\{(S_h, V_h, E_h, I_h, Q, T, R, S_b, V_b, E_b, I_b) \in R_+^{11}; N_h(t) \leq \frac{\Lambda_h}{\mu_h}, N_b(t) \leq \frac{\Lambda_b}{\mu_b}\right\} QED.$$

Furthermore, whenever $N_h > \frac{\Lambda_h}{\mu_h}$, then by (2.4), $\frac{dN_h}{dt} < 0$, similarly, whenever $N_b > \frac{\Lambda_b}{\mu_b}$, then $\frac{dN_b}{dt} < 0$. This means that the host population reduces asymptotically to its carrying capacity. Thus, every solution with initial condition in R_+^{11} remains in that region Ω for $t > 0$, which is a positively invariant set under the flow induced by model (2.1). Hence, the system (2.1) is mathematically well-posed in the interior of the domain of Ω.

Positivity of solutions

Definition 1. *: The solution to model* (2.1) *is said to be positive if all the state variables in the model take non-negative values.*

For model (2.1) to be epidemiologically meaningful, it is important to prove that all its state variables are non-negative for all time t. It has to be shown that solution of model (2.1) with positive initial data remains positive for all time $t > 0$. The result is presented below.

Lemma 1. *:* Let the initial value of the system in (2.1) be $\{(S_h(0), V_h(0), E_h(0), I_h(0), Q(0), T(0), R(0), S_b(0), V_b(0), E_b(0), I_b(0)) \geq 0\} \in \Omega$.
Then, the solution set $\{S_h(t), V_h(t), E_h(t), I_h(t), Q(t), T(t), R(t), S_b(t), V_b(t)), E_b(t), I_b(t)\}$ of (2.1) is positive for all $t > 0$.

Proof. Consider the first equation in (2.1), that is,

$$\frac{dS_h}{dt} = \Lambda_h - \beta S_h I_b - \beta_h S_h I_h - (\mu_h + \rho + \varepsilon)S_h + \alpha R + \psi_h V_h. \ \ such\ that\ \ \beta \in [0,1)\ \ and\ \ \beta_h \leq \frac{\Lambda_h}{S_h I_h},$$

then

$$\frac{dS_h}{dt} \geq -(\mu_h + \rho + \varepsilon)S_h,$$

implying that

Article DOI: 10.52589/AJMSS-KSUGFI1Z
DOI URL: https://doi.org/10.52589/AJMSS-KSUGFI1Z

African Journal of Mathematics and Statistics Studies
ISSN: 2689-5323
Volume 8, Issue 3, 2025 (pp. 136-161)
www.abjournals.org

$$\int \frac{1}{S_h} dS_h \geq -(\mu_h + \rho + \varepsilon) \int dt.$$

i.e.,

$$S_h(t) \geq Ae^{-(\mu_h+\rho+\varepsilon)t}, \quad where\ A\ is\ a\ constant$$

Setting t = 0 and applying the initial conditions, yields

$$S_h(t) \geq S_h(0)e^{-(\mu_h+\rho+\varepsilon+)t} \geq 0, \ \ since \ \ (\mu_h + \rho + \varepsilon) > 0. \qquad (2.10)$$

Hence, S_h is always positive for $t > 0$. Similarly, other state variables in (2.1) are obtained as follows:

$$V_h(t) \geq V_h(0)e^{-(\psi_h+\mu_h)t} \geq 0, \ \ since \ \ (\psi_h + \mu_h) > 0. \qquad (2.11)$$

$$E_h(t) \geq E_h(0)e^{-(\mu_h+\sigma_h)t} \geq 0, \ \ since \ \ (\mu_h + \sigma_h) > 0. \qquad (2.12)$$

$$I_h(t) \geq I_h(0)e^{-(k+\gamma_1+\eta+\mu_h+\phi_h)t} \geq 0, \ \ since \ \ (k + \gamma_1 + \eta + \mu_h + \phi_h) > 0. \qquad (2.13)$$

$$Q(t) \geq Q(0)e^{-(\delta+\mu_h+\phi)t} \geq 0, \ \ since \ \ (\delta + \mu_h + \phi) > 0. \qquad (2.14)$$

$$T(t) \geq T(0)e^{-(\mu_h+\gamma_2)t} \geq 0, \ \ since \ \ (\mu_h + \gamma_2) > 0. \qquad (2.15)$$

$$R(t) \geq R(0)e^{-(\mu_h+\alpha)t} \geq 0, \ \ since \ \ (\mu_h + \alpha) > 0. \qquad (2.16)$$

$$S_b(t) \geq S_b(0)e^{-(\mu_b+\rho_b)t} \geq 0, \ \ since \ \ (\mu_b + \rho_b) > 0. \qquad (2.17)$$

$$V_b(t) \geq V_b(0)e^{-(\psi_b+\mu_b)t} \geq 0, \ \ since \ \ (\psi_b + \mu_b) > 0. \qquad (2.18)$$

$$E_b(t) \geq E_b(0)e^{-(\sigma_b+\mu_b)t} \geq 0, \ \ since \ \ (\sigma_b + \mu_b) > 0. \qquad (2.19)$$

$$I_b(t) \geq I_b(0)e^{-(\mu_b+\phi_b)t} \geq 0, \ \ since \ \ (\mu_b + \phi_b) > 0. \qquad (2.20)$$

The inequalities in (2.10) to (2.20) show that the variables $S_h(t)$, $V_h(t)$,$E_h(t)$, $I_h(t)$,Q(t), T(t), R(t), $S_b(t)$, $V_b(t)$, $E_b(t)$ and $I_b(t)$ are positive for all $t > 0$. Hence, the proof of Lemma 1 is completed QED.

EXISTENCE OF EQUILIBRIUM STATES

Let E_h and E_b denote the equilibrium points of the respective components $E_h(S_h, V_h, E_h, I_h, Q, T, R) = \Omega_h$ and $E_b(S_b, V_b, E_b, I_b) = \Omega_b$ of the system described by (2.1). The equilibrium states are obtained by invoking the conditions

$$\frac{dS_h}{dt} = \frac{dV_h}{dt} = \frac{dE_h}{dt} = \frac{dI_h}{dt} = \frac{dQ}{dt} = \frac{dT}{dt} = \frac{dR}{dt} = 0, and\ \frac{dS_b}{dt} = \frac{dV_b}{dt} = \frac{dE_b}{dt} = \frac{dI_b}{dt} = 0. \qquad (3.1)$$

The equilibrium states are obtained as follows:

$$\wedge_h - \beta S_h I_b - \beta_h S_h I_h - (\mu_h + \rho + \varepsilon)S_h + \alpha R + \psi_h V_h = 0\ \rho S_h - (\psi_h + \mu_h)V_h = 0\ \beta S_h I_b + \beta_h S_h I_h - (\mu_h + \sigma_h)E_h =$$

Article DOI: 10.52589/AJMSS-KSUGFI1Z
DOI URL: https://doi.org/10.52589/AJMSS-KSUGFI1Z

African Journal of Mathematics and Statistics Studies
ISSN: 2689-5323
Volume 8, Issue 3, 2025 (pp. 136-161)
www.abjournals.org

$$0\ \sigma_h E_h - (k+\gamma_1+\eta+\mu_h+\phi_h)I_h = 0\ kI_h - (\delta+\mu_h+\phi)Q = 0\ \eta I_h + \delta Q - (\mu_h+\gamma_2)T = 0\ \gamma_2 T + \gamma_1 I_h + \varepsilon S_h - (\mu_h+\alpha)R = 0\ \wedge_b - \beta_b S_b I_b - (\mu_b+\rho_b)S_b + \psi_b V_b = 0\ \rho_b S_b - (\psi_b+\mu_b)V_b = 0\ \beta_b S_b I_b - (\sigma_b+\mu_b)E_b = 0\ \sigma_b E_b - (\mu_b+\phi_b)I_b = 0.\} \quad (3.2)$$

Then by direct calculation, it can be shown that (3.2) has the following two equilibria states in R_+^{11}:
Disease-free equilibrium $E_{b,h}^+ = (S_h^+, V_h^+, E_h^+, I_h^+, Q^+, T^+, R^+, S_b^+, V_b^+, E_b^+, I_b^+) \in \Omega_{h,b}^+$ and
Endemic equilibrium $E_{h,b}^* = (S_h^*, V_h^*, E_h^*, I_h^*, Q^*, T^*, R^*, S_b^*, V_b^*, E_b^*, I_b^*) \in \Omega_{h,b}^*$

Disease-Free equilibrium state

The disease-free equilibrium (DFE) state is the state at which there are no infections in the population or total eradication of the disease.
Solving the system of equations (3.2) simultaneously, the disease-free equilibrium state for both human and bird population of the avian influenza model in (2.1) is obtained as below.

$$E_{b,h}^+ = (S_h^+, V_h^+, E_h^+, I_h^+, Q^+, T^+, R^+, S_b^+, V_b^+, E_b^+, I_b^+) = \left(\frac{(\psi_h+\mu_h)(\mu_h+\alpha)\wedge_h}{\mu_h[(\mu_h+\alpha+\varepsilon)(\mu_h+\psi_h)+\rho(\mu+\alpha)]}, \frac{\wedge_h \rho(\mu_h+\alpha)}{\mu_h[(\mu_h+\alpha+\varepsilon)(\mu_h+\psi_h)+\rho(\mu+\alpha)]}, 0,0,0,0,\right.$$
$$\left.\frac{\wedge_h\varepsilon(\psi_h+\mu_h)}{\mu_h[(\mu_h+\alpha+\varepsilon+)(\mu_h+\psi_h)+\rho(\mu+\alpha)]}, \frac{\wedge_b(\psi_b+\mu_b)}{\mu_b(\psi_b+\mu_b+\rho_b)}, \frac{\rho_b\wedge_b}{\mu_b(\psi_b+\mu_b+\rho_b)}, 0,0\right). \quad (3.3)$$

Endemic equilibrium state

Endemic-equilibrium state is the state where the disease cannot be totally eradicated but persists in the population. Then, all the state variables in (2.1) must not be zero at the equilibrium state, i.e., $E_{(b,h)}^* = (S_h^*, V_h^*, E_h^*, I_h^*, Q^*, T^*, R^*, S_b^*, V_b^*, E_b^*, I_b^*)\Omega \neq (0,0,0,0,0,0,0,0,0,0,0)$.

$$\wedge_h - \beta S_h^* I_b^* - \beta_h S_h^* I_h^* - (\mu_h+\rho+\varepsilon)S_h^* + \alpha R^* + \psi_h V_h^* = 0, \rho S_h - (\psi_h+\mu_h)V_h^* = 0, \beta S_h^* I_b^* + \beta_h S_h^* I_h^* - (\mu_h+\sigma_h)E_h^* = 0\ \sigma_h E_h^* - (k+\gamma_1+\eta+\mu_h+\phi_h)I_h^* = 0\ kI_h^* - (\delta+\mu_h+\phi)Q^* = 0\ \eta I_h^* + \delta Q^* - (\mu_h+\gamma_2)T^* = 0\ \gamma_2 T^* + \gamma_1 I_h^* + \varepsilon S_h^* - (\mu_h+\alpha)R^* = 0\ \wedge_b - \beta_b S_b^* I_b^* - (\mu_b+\rho_b)S_b^* + \psi_b V_b^* = 0\ \rho_b S_b^* - (\psi_b+\mu_b)V_b^* = 0\ \beta_b S_b^* I_b^* - (\sigma_b+\mu_b)E_b^* = 0\ \sigma_b E_b^* - (\mu_b+\phi_b)I_b^* = 0\} \quad (3.4)$$

To obtain the endemic equilibrium state, each equation (3.4) is equated to zero and solved simultaneously in terms of R_0 following the idea used in [2, 5, 6, 9, 29, 32] .

$$S_b^* = \frac{S_b^+}{R_0^b}, \quad (3.5)$$

where $S_b^+ = \frac{\wedge_b(\psi_b+\mu_b)}{\mu_b(\psi_b+\mu_b+\rho_b)}$, and $R_0^b = \frac{\beta_b\wedge_b\sigma_b(\psi_b+\mu_b)}{\mu_b(\psi_b+\mu_b+\rho_b)(\mu_b+\phi_b)(\sigma_b+\mu_b)}$

Article DOI: 10.52589/AJMSS-KSUGFI1Z
DOI URL: https://doi.org/10.52589/AJMSS-KSUGFI1Z

African Journal of Mathematics and Statistics Studies
ISSN: 2689-5323
Volume 8, Issue 3, 2025 (pp. 136-161)
www.abjournals.org

$$\Rightarrow S_b^* = \frac{\wedge_b\,(\psi_b + \mu_b)}{\mu_b(\psi_b + \mu_b + \rho_b)R_0^b}$$

Substituting these expressions into the system (3.4), yield:

$$E^* = \{S_h^* = \frac{\wedge_h(\psi_h+\mu_h)(\mu_h+\alpha)}{\mu_h[(\mu_h+\alpha+\varepsilon)(\mu_h+\psi_h)+\rho(\mu+\alpha)]R_0^h}\ V_h^* = \frac{\wedge_h\rho(\mu_h+\alpha)}{\mu_h[(\mu_h+\alpha+\varepsilon)(\mu_h+\psi_h)+\rho(\mu+\alpha)]R_0^h}\ E_h^* = \frac{\beta\wedge_h\mu_b(\psi_h+\mu_h)(\mu_h+\alpha)(\psi_b+\mu_b+\rho_b)[R_0^b-1][A+\beta_h\sigma_h\wedge_h(\psi_h+\mu_h)(\mu_h+\alpha)]}{\beta_b(\psi_b+\mu_b)(\mu_h+\sigma_h)BA}\ I_h^* = \frac{\sigma_h\beta\wedge_h\mu_b(\psi_h+\mu_h)(\mu_h+\alpha)(\psi_b+\mu_b+\rho_b)[R_0^b-1]}{\beta_b(\psi_b+\mu_b)[AR_0^h-\wedge_h\sigma_h\beta_h(\psi_h+\mu_h)(\mu_h+\alpha)]}\ T^* = \frac{\sigma_h\beta\wedge_h\mu_b(\psi_h+\mu_h)(\mu_h+\alpha)(\psi_b+\mu_b+\rho_b)[R_0^b-1][\eta(\delta+\mu_h+\phi)+\delta k]}{\beta_b(\mu_h+\gamma_2)(\delta+\mu_h+\phi)(\psi_b+\mu_b)[AR_0^h-\wedge_h\sigma_h\beta_h(\psi_h+\mu_h)(\mu_h+\alpha)]}\ Q^* = \frac{\sigma_h\beta\wedge_h\mu_b k(\psi_h+\mu_h)(\mu_h+\alpha)(\psi_b+\mu_b+\rho_b)[R_c^b-1]}{\beta_b(\delta+\mu_h+\phi)(\psi_b+\mu_b)[AR_0^h-\wedge_h\sigma_h\beta_h(\psi_h+\mu_h)(\mu_h+\alpha)]}\ R^* = \frac{B(\gamma_2+)\sigma_h\beta\wedge_h\mu_b(\psi_h+\mu_h)(\psi_b+\mu_b+\rho_b)[R_0^b-1]C+(\mu_h+\gamma_2)(\delta+\mu_h+\phi)A[B+\psi_b+\mu_b]}{\beta_b(\mu_h+\gamma_2+)(\delta+\mu_h+\phi)(\psi_b+\mu_b)A\wedge_h(\varepsilon+)(\psi_h+\mu_h)}\ S_b^* = \frac{\wedge_b(\psi_b+\mu_b)}{\mu_b(\psi_b+\mu_b+\rho_b)R_0^b}\ V_b^* = \frac{\rho_b\wedge_b}{\mu_b(\psi_b+\mu_b+\rho_b)R_0^b}\ E_b^* = \frac{\mu_b(\mu_b+\phi_b)(\psi_b+\mu_b+\rho_b)[R_0^b-1]}{\beta_b\sigma_b(\psi_b+\mu_b)}\ I_b^* = \frac{\mu_b(\psi_b+\mu_b+\rho_b)[R_0^b-1]}{\beta_b(\psi_b+\mu_b)},$$

(3.6)

where,

$$A = \big[\mu_h(\mu_h+\sigma_h)(k++\gamma_1+\eta+\mu_h+\phi_h)[(\mu_h+\alpha+\varepsilon)(\mu_h+\psi_h)+\rho(\mu+\alpha)]R_0^h - \wedge_h\sigma_h\beta_h(\psi_h+\mu_h)(\mu_h+\alpha)\big]B = \mu_h[(\mu_h+\alpha+\varepsilon)(\mu_h+\psi_h)+\rho(\mu+\alpha)]R_0^h$$

$C = [\eta(\delta+\mu_h+\phi)+\delta k]$.

Thus, if $R_0^b > 1$ and $R_0^h > 1$, then, $I_h^* > 0$ and $I_b^* > 0$ and model [1] has endemic equilibrium point given by $E^* = (S_h^*, V_h^*, E_h^*, I_h^*, T^*, Q^*, R^*, S_b^*, V_b^*, E_b^*, I_b^*)$ in the presence of infection (i. e $I_{b,h} \neq 0$). Therefore, to ensure the existence of a positive endemic-equilibrium, we require $R_0^{h,b} > 1$. Substituting $R_0^{b,h} > 1$ into each component in (33) yield $S_h^*, > 0, V_h^*, > 0, E_h^*, > 0, I^*h, > 0, T^*, > 0, Q^*, > 0, R^*, > 0, S_b^*, > 0, V_b *, > 0, E_b^*, > 0$ and $I_b^* > 0$. Thus , the endemic-equilibrium E^* is positive and $I_{b,h}^* > 0$ when $R_0^{b,h} > 1$. This is the condition for the existence and uniqueness of the endemic-equilibrium for the system [1]. The proof of Uniqueness of the endemic equilibrium.

Basic Reproductive Number

In this section, we compute the basic reproductive number R_0 using the next generation approach as described in [15, 31].
For any epidemic model, the basic reproduction number is the average number of secondary infectious cases produced by a single infection in the total susceptible population. The basic reproduction number is calculated by $R_0 = \rho(FV^{-1})$ where ρ is the spectral radius of the matrix FV^{-1}, F and V are the matrices of new infection terms and the remaining transmission terms respectively given by.

Article DOI: 10.52589/AJMSS-KSUGFI1Z
DOI URL: https://doi.org/10.52589/AJMSS-KSUGFI1Z

African Journal of Mathematics and Statistics Studies
ISSN: 2689-5323
Volume 8, Issue 3, 2025 (pp. 136-161)
www.abjournals.org

$F_i = (\beta S_h I_h + \beta_h S_h I_h \ \ 0 \ \ 0 \ \ 0 \ \ \beta_b S_b I_b \ \ 0 \ \ ), V_i = ((\mu_h + \sigma_h)E_h \ \ (k + \gamma_1 + \eta + \mu_h + \phi_h)I_h - \sigma_h E_h \ \ (\delta + \mu_h + \phi)Q - (k+)I_h \ \ (\mu_h + \gamma_2 +)T - \eta I_h - \delta Q \ \ (\sigma_b + \mu_b)E_b \ \ (\mu_b + \phi_b)I_b - \sigma_b E_b \ ),$ (3.7)

Jacobian matrices of F and V at the DFE are obtained as

$$F = (0\ \beta_h S_h\ 0\ 0\ 0\ \beta S_h \ \ 0\ 0\ 0\ 0\ 0\ 0 \ \ 0\ 0\ 0\ 0\ 0\ 0 \ \ 0\ 0\ 0\ 0\ 0\ 0 \ \ 0\ 0\ 0\ 0\ 0\ \beta_b S_b \ \ 0\ 0\ 0\ 0\ 0\ 0 \quad) \tag{3.8}$$

and

$$V = ((\mu_h + \sigma_h)\ 0\ 0\ 0\ 0\ 0 \ \ -\sigma_h\ (k + \gamma_1 + \eta + \mu_h + \phi_h)\ 0\ 0\ 0 \ \ 0\ -(k)\ (\delta + \mu_h + \phi)\ 0\ 0\ 0 \ \ 0\ -\eta \ \ -\delta\ (\mu_h + \gamma_2 +)\ 0\ 0 \ \ 0\ 0\ 0\ 0\ (\sigma_b + \mu_b)\ 0 \ \ 0\ 0\ 0\ 0 \ \ -\sigma_b \ \ \mu_b + \phi_b\ ) \tag{3.9}$$

$$FV^{-1} = \left(\beta_h S_h \vartheta_1 \ \beta_h S_h \vartheta_2 \ 0\ 0\ \beta S_h \vartheta_8 \ \frac{\beta S_h}{\mu_b + \phi_b} \ \ 0\ 0\ 0\ 0\ 0\ 0 \ \ 0\ 0\ 0\ 0\ 0\ 0 \ \ 0\ 0\ 0\ 0\ 0\ 0 \ \ 0\ 0\ 0\ 0\ \beta_b S_b \vartheta_8 \ \frac{\beta_b S_b}{\mu_b + \phi_b} \ \ 0\ 0\ 0\ 0\ 0\ 0 \right)$$

Solving FV^{-1}, the effective reproductive number for bird population, R_0^b and human population, R_0^h are respectively obtained as

where

$$\vartheta_1 = \frac{\sigma_h}{(\mu_h+\sigma_h)(k+\gamma_1+\eta+\mu_h+\phi_h)}, \vartheta_2 = \frac{1}{(k+\gamma_1+\eta+\mu_h+\phi_h)}, \vartheta_3 = \frac{k\sigma_h}{(\mu_h+\sigma_h)(k+\gamma_1+\eta+\mu_h+\phi_h)(\delta+\mu_h+\phi)}, \vartheta_4 = \frac{k}{(k+\gamma_1+\eta+\mu_h+\phi_h)(\delta+\mu_h+\phi)}, \vartheta_5 = \frac{\sigma_h(\eta\,\delta+\eta\,\mu_h+\eta\,\phi-\delta\,k)}{(\mu_h+\sigma_h)(k+\gamma_1+\eta+\mu_h+\phi_h)(\delta+\mu_h+\phi)(\mu_h+\gamma_3)}, \vartheta_6 = \frac{\eta\,\delta+\eta\,\mu_h+\eta\,\phi-\delta\,k}{(k+\gamma_1+\eta+\mu_h+\phi_h)(\delta+\mu_h+\phi)(\mu_h+\gamma_3)}, \vartheta_7 = \frac{\delta}{(\delta+\mu_h+\phi)(\mu_h+\gamma_3)}, \vartheta_8 = \frac{\sigma_b}{(\sigma_b+\mu_b)(\mu_b+\phi_b)} \tag{3.11}$$

$$R_0^{b,h} = \rho(FV^{-1}) = max\left\{\frac{\beta_b S_b \sigma_b}{(\sigma_b+\mu_b)(\mu_b+\phi_b)}, \frac{\beta_h S_h \sigma_h}{(k++\gamma_1+\eta+\mu_h+\phi_h)(\mu_h+\sigma_h)}\right\} \tag{3.12}$$

After substituting, $S_b = \frac{\wedge_b(\psi_b+\mu_b)}{\mu_b(\psi_b+\mu_b+\rho_b)}$ and $S_h = \frac{\wedge_h(\mu_h+\psi_h)(\mu_h+\alpha)}{\mu_h[(\mu_h+\alpha+\varepsilon)(\psi_h+\mu_h)+\rho\,(\mu_h+\alpha)]}$ into (3.12) we have $R_0^b = \frac{\beta_b \wedge_b \sigma_b(\psi_b+\mu_b)}{\mu_b(\psi_b+\mu_b+\rho_b)(\mu_b+\phi_b)(\sigma_b+\mu_b)}$ and

$$R_0^h = \frac{\beta_h \wedge_h \sigma_h(\psi_h + \mu_h)(\mu_h + \alpha)}{\mu_h[(\mu_h + \alpha + \varepsilon)(\psi_h + \mu_h) + \rho\,(\mu_h + \alpha)](\mu_h + \sigma_h)(k + \gamma_1 + \eta + \mu_h + \phi_h)}$$

Hence, the interface of basic reproductive number for both bird and human populations is obtained as

$$R_0^{b,h} = \frac{\beta_b \wedge_b \sigma_b \beta_h \wedge_h \sigma_h(\psi_b+\mu_b)(\mu_h+\psi_h)(\mu_h+\alpha)}{G} \tag{3.13}$$

$$G = \mu_b(\psi_b + \mu_b + \rho_b)(\sigma_b + \mu_b)(\mu_b + \phi_b)\mu_h[(\mu_h + \alpha + \varepsilon)(\psi_h + \mu_h) + \rho\,(\mu_h + \alpha)](\mu_h + \sigma_h)(k + \gamma_1 + \eta + \mu_h + \phi_h)$$

Remark 1. *Epidemiologically,*

Article DOI: 10.52589/AJMSS-KSUGFI1Z
DOI URL: https://doi.org/10.52589/AJMSS-KSUGFI1Z

African Journal of Mathematics and Statistics Studies
ISSN: 2689-5323
Volume 8, Issue 3, 2025 (pp. 136-161)
www.abjournals.org

- *if* $R_0^{b,h} < 1$*, the occurrence of the disease will decrease and eventually be eliminated.*
- *if* $R_0^{b,h} = 1$*, the disease's occurrence will remain constant.*
- *if* $R_0^{b,h} > 1$ *the occurrence of the disease will increase and persist.*

Local stability of the disease-free equilibrium state

To determine the stability or otherwise of the system (2.1) at the disease-free equilibrium point E^+, the behavior of the model population near the equilibrium point is examined to determine the satisfaction of the conditions that must be met for the disease-free equilibrium state to be stable and at the same time to be totally eradicated from the population.

Theorem 2: The *disease-free equilibrium point* E^+ *of the model system (2.1) is locally asymptotically stable if* $R_0^{b,h} < 1$ *and unstable if* $R_0^{b,h} > 1$

Lemma 2: Subject *to the assumptions of theorem 2, the disease-free equilibrium point* E^+ *is locally asymptotically stable if and only if* $tr(J_{E^+}) < 0\ det(J_{E^+}) > 0$*, and unstable if* $R_0^{b,h} > 1$ *for* $tr(J_{E^+}) > 0$ *and* $det(J_{E^+}) < 0$ *following.*

Proof. The proof of the theorem can be established by constructing a Jacobian matrix for the model system (2.1) evaluated at the DFE (E^+).
Let, $\Psi_1 = (\mu_h + \rho + \varepsilon), \Psi_2 = (k + \gamma_1 + \eta + \mu_h + \phi_h), \Psi_3 = (\delta + \mu_h + \phi), \Psi_4 = (\mu_h + \gamma_2+), \Psi_5 = (\mu_b + \rho_b)$
At the disease-free equilibrium point E^+, the Jacobian matrix

$$J_{E^+} = (-\beta I_b^+ - \beta_h I_h^+ - \Psi_1\ \psi_h\ 0\ -\beta_h S_h^+\ 0\ 0\ \alpha\ 0\ 0\ 0\ -\beta S_h^+\ \rho\ -(\psi_h + \mu_h)\ 0\ 0\ 0\ 0\ 0\ 0\ 0\ 0\ 0\ \beta I_b^+ + \beta_h I_h^+\ 0\ -(\mu_h + \sigma_h)\ \beta_h S_h^+\ 0\ 0\ 0\ 0\ 0\ 0\ \beta S_h^+\ 0\ 0\ \sigma_h\ - \Psi_2\ 0\ 0\ 0\ 0\ 0\ 0\ 0\ 0\ 0\ 0\ 0\ (k)\ -\Psi_3\ 0\ 0\ 0\ 0\ 0\ 0\ 0\ 0\ 0\ \eta\ \delta\ -\Psi_4\ 0\ 0\ 0\ 0\ 0\ (\varepsilon+)\ 0\ 0\ \gamma_1\ 0\ (\gamma_2+)\ - (\mu_h + \alpha)\ 0\ 0\ 0\ 0\ 0\ 0\ 0\ 0\ 0\ 0\ 0\ 0\ -\beta_b I_b^+ - \Psi_5\ \psi_b\ 0\ -\beta_b S_b^+\ 0\ 0\ 0\ 0\ 0\ 0\ 0\ \rho_b\ -(\psi_b + \mu_b)\ 0\ 0\ 0\ 0\ 0\ 0\ 0\ 0\ 0\ \beta_b I_b^+\ -(\sigma_b + \mu_b)\ 0\ \beta_b S_b^+\ 0\ 0\ 0\ 0\ 0\ 0\ 0\ 0\ 0\ \sigma_b\ -(\mu_b + \phi_b)\ ) \quad (3.14)$$

After substituting $I_b^+ = I_h^+ = 0$ into (3.14), this will result in

$$J_{E^+} = (-A_1\ \psi_h\ 0\ -L\ 0\ 0\ \alpha\ 0\ 0\ 0\ -P\ \rho\ -A_2\ 0\ 0\ 0\ 0\ 0\ 0\ 0\ 0\ 0\ 0\ 0\ 0\ -A_3\ L\ 0\ 0\ 0\ 0\ 0\ 0\ P\ 0\ 0\ - \sigma_h\ -A_4\ 0\ 0\ 0\ 0\ 0\ 0\ 0\ 0\ 0\ 0\ 0\ 0\ A_5\ -A_6\ 0\ 0\ 0\ 0\ 0\ 0\ 0\ 0\ 0\ \eta\ \delta\ -A_7\ 0\ 0\ 0\ 0\ 0\ A_8\ 0\ 0\ \gamma_1\ 0\ A_9\ - A_{10}\ 0\ 0\ 0\ 0\ 0\ 0\ 0\ 0\ 0\ 0\ 0\ 0\ 0\ -B_1\ \psi_b\ 0\ -M\ 0\ 0\ 0\ 0\ 0\ 0\ 0\ \rho_b\ -B_2\ 0\ 0\ 0\ 0\ 0\ 0\ 0\ 0\ 0\ 0\ 0\ 0\ - B_3\ M\ 0\ 0\ 0\ 0\ 0\ 0\ 0\ 0\ 0\ \sigma_b\ -B_4\ ) \quad (3.15)$$

We now want to show that Matrix J_{E^+} in (3.15) is stable if its trace is negative, i.e., $tr(J_{E^+}) < 0$ and its determinant is non-negative, i.e., $det(J_{E^+}) > 0$. The trace of the matrix J_{E^+} is obtained as:

$$\begin{aligned} tr(J_{E^+}) &= -A_1 - A_2 - A_3 - A_4 - A_6 - A_7 - A_{10} - B_1 - B_2 - B_3 - B_4 \\ &= -(A_1 + A_2 + A_3 + A_4 + A_6 + A_7 + A_{10} + B_1 + B_2 + B_3 + B_4) \\ &= -(\alpha + k + \psi_h + \rho + \varepsilon + 7\,\mu_h + u_1 + 4\,\mu_b + \psi_b + \eta + \sigma_h + \gamma_1 + \phi_h + \phi \\ &+ \delta + \gamma_2 + \rho_b + \sigma_b + \phi_b) \ \therefore \quad tr(J^+) \\ &< 0\ since\ each\ of\ the\ quantities\ enclosed\ in\ the\ brackets\ is\ non - negative. \end{aligned}$$

Article DOI: 10.52589/AJMSS-KSUGFI1Z
DOI URL: https://doi.org/10.52589/AJMSS-KSUGFI1Z

African Journal of Mathematics and Statistics Studies
ISSN: 2689-5323
Volume 8, Issue 3, 2025 (pp. 136-161)
www.abjournals.org

Also, the determinant of matrix J_{E^+} is generated as

$$det(J_{E^+}) = A_6A_7(A_3A_4 + L\sigma_h)(B_1B_2 - \rho_b\psi_b)(B_3B_4 - M\sigma_b)(A_{10}\rho\,\psi_h + A_8\alpha\,A_2 - A_{10}A_2A_1)$$

$Hence,\quad det(J_{E^+}) > 0\ provided\ \rho_b\psi_b < B_1B_2, M\sigma_b < B_3B_4\ \ and\ \ A_{10}A_2A_1 < (A_{10}\rho\psi + A_8A_2\alpha)$,
where
$A_1 = (\mu_h + \rho + \varepsilon), A_2 = (\psi_h + \mu_h), A_3 = (\mu_h + \sigma_h), A_4 = (k + \gamma_1 + \eta + \mu_h + \phi_h), A_5 = k, A_6 = (\delta + \mu_h + \phi), A_7 = (\mu_h + \gamma_2), A_8 = \varepsilon, A_9 = \gamma_2, A_{10} = (\mu_h + \alpha), B_1 = (\mu_b + \rho_b), B_2 = (\psi_b + \mu_b), B_3 = (\sigma_b + \mu_b), B_4 = (\mu_b + \phi_b), L = \frac{C_1}{C_2}, P = \frac{C_3}{C_2}, M = \frac{d_1}{d_2}, C_1 = \beta_h \wedge_h (\psi_h + \mu_h)(\mu_h + \alpha), C_2 = \mu_h[(\mu_h + \alpha + \varepsilon)(\mu_h + \psi_h) + \rho(\mu + \alpha)], C_3 = \beta \wedge_h (\psi_h + \mu_h)(\mu_h + \alpha), d_1 = \beta_b \wedge_b (\psi_b + \mu_b), d_2 = \mu_b(\psi_b + \mu_b + \rho_b).$

$$det(J_{E^+}) = A_6A_7A_3A_4B_1B_2[B_1B_2 - \rho_b\psi_b][A_{10}\rho\,\psi_h + A_2A_8\alpha - A_{10}A_2A_1]\left[1 + R_0^h\right]\left[1 - R_0^b\right]$$

Hence, the result proves that the disease-free equilibrium point is locally asymptotically stable. Biologically, this means that the disease will die out.

Global stability of disease-free equilibrium

In this subsection, global stability of the disease-free equilibrium (E^+) will be ascertained. The result is obtained by means of the Lyapunov function in [5, 6, 32].

Theorem 3. *For $R_0 \le 1$, the disease-free equilibrium of the system* (2.1) *is stable globally asymptotically if $S_h = S_h^0, S_b = S_b^0$ and unstable if $R_0 > 1$.*

$$\begin{aligned}
V(t) &= d_1(S_h - S_h^0) + d_2V_h + d_3E_h + d_4I_h + d_5Q + d_6T + d_7R + d_8(S_b - S_b^0) + d_9V_b \\
&\quad + d_{10}E_b + d_{11}I_b, \dot{V}(t) \\
&= d_1\dot{S_h} + d_2\dot{V_h} + d_3\dot{E_h} + d_4\dot{I_h} + d_5\dot{Q} + d_6\dot{T} + d_7\dot{R} + d_8\dot{S_b} + d_9\dot{V_b} + d_{10}\dot{E_b} \\
&\quad + d_{11}\dot{I_b} \\
&= d_1[\wedge_h - \beta S_hI_b - \beta_hS_hI_h - (\mu_h + \rho + \varepsilon)S_h + \alpha R + \psi_hV_h] + d_2[\rho S_h - (\psi_h \\
&\quad + \mu_h)V_h] + d_3[\beta S_hI_b + \beta_hS_hI_h - (\mu_h + \sigma_h)E_h] + d_4\sigma_hE_h - (k + \gamma_1 + \eta + \mu_h \\
&\quad + \phi_h)I_h + d_5kI_h - (\delta + \mu_h + \phi)Q + d_6\eta I_h + \delta Q - (\mu_h + \gamma_2)T + d_7\gamma_2T \\
&\quad + \gamma_1I_h + \varepsilon S_h - (\mu_h + \alpha)R + d_8 \wedge_b - \beta_bS_bI_b - (\mu_b + \rho_b)S_b + \psi_bV_b \\
&\quad + d_9\rho_bS_b - (\psi_b + \mu_b)V_b + d_{10}\beta_bS_bI_b - (\sigma_b + \mu_b)E_b + d_{11}\sigma_bE_b - (\mu_b \\
&\quad + \phi_b)I_b \\
&= (d_3 - d_1)[\beta I_b + \beta_hI_h]S_h + (d_1 - d_2)(\psi_hV_h) + (d_7 - d_1)\varepsilon S_h + (d_2 \\
&\quad - d_1)\rho S_h + (d_4 - d_3)\sigma_hE + (d_1 - d_7)(\alpha R) + (d_5 - d_4)kI_h + (d_6 - d_4)\eta I_h \\
&\quad + (d_7 - d_4)\gamma_1I_h + (d_6 - d_5)\delta Q + (d_7 - d_6)\gamma_2T + d_1 \wedge_h - d_1(\mu_h)S_h \\
&\quad - d_2\mu_hV_h - d_3\mu_hE_h - d_4(\mu_h + \phi_h)I_h - d_5(\mu_h + \phi)Q - d_6\mu_hT - d_7\mu_hR \\
&\quad + d_8 \wedge_b + (d_{10} - d_8)(\beta_bS_bI_b) + (d_9 - d_8)(\rho_bS_b) + (d_{11} - d_{10})\sigma_bE_b + (d_8 \\
&\quad - d_9)(\psi_b)V_b - d_8\mu_bS_b - d_9\mu_bV_b - d_{10}\mu_bE_b - d_{11}(\mu_b + \phi)I_b.
\end{aligned}$$

From (3.3), $S_h^+ = \frac{(\psi_h+\mu_h)(\mu_h+\alpha)\wedge_h}{\mu_h[(\mu_h+\alpha+\varepsilon)(\mu_h+\psi_h)+\rho(\mu+\alpha)]} \Longrightarrow \wedge_h = \frac{\mu_h[(\mu_h+\alpha+\varepsilon)(\mu_h+\psi_h)+\rho(\mu+\alpha)]S_h^+}{(\psi_h+\mu_h)(\mu_h+\alpha)}$ and $S_b^+ = \frac{\wedge_b(\psi_b+\mu_b)}{\mu_b(\psi_b+\mu_b+\rho_b)}$

Article DOI: 10.52589/AJMSS-KSUGFI1Z
DOI URL: https://doi.org/10.52589/AJMSS-KSUGFI1Z

African Journal of Mathematics and Statistics Studies
ISSN: 2689-5323
Volume 8, Issue 3, 2025 (pp. 136-161)
www.abjournals.org

$\Longrightarrow \Lambda_b = \frac{\mu_b(\psi_b+\mu_b+\rho_b)S_b^+}{(\psi_b+\mu_b)}$

Thus,

$$\dot{V}(t) = -(d_1-d_3)[\beta I_b + \beta_h I_h]S_h + (d_2-d_1)\psi_h V_h + (d_1-d_7)\varepsilon S_h + (d_1-d_2)\rho S_h + (d_3-d_4)\sigma_h E + (d_7-d_1)\alpha R + (d_4-d_5)kI_h + (d_4-d_5)\eta I_h + (d_4-d_7)\gamma_1 I_h + (d_5-d_6)\delta Q + (d_6-d_7)\gamma_2 T + d_1\mu_h\left[\frac{(\psi_h+\mu_h)(\mu_h+\alpha)S_h-[(\mu_h+\alpha+\varepsilon)(\mu_h+\psi_h)+\rho(\mu+\alpha)]S_h^+}{(\psi_h+\mu_h)(\mu_h+\alpha)}\right] + d_2\mu_h V_h + d_3\mu_h E_h - d_4(\mu_h+\phi_h)I_h - d_5(\mu_h+\phi)Q + d_6\mu_h T + d_7\mu_h R + d_8\mu_b\left[\frac{(\psi_b+\mu_b)S_b-(\psi_b+\mu_b+\rho_b)S_b^+}{(\psi_b+\mu_b)}\right] + (d_8-d_{10})(\beta_b S_b I_b) + (d_8-d_9)(\rho_b S_b) + (d_{10}-d_{11})\sigma_b E_b + (d_9-d_8)(\psi_b)V_b + d_9\mu_b V_b + d_{10}\mu_b E_b + d_{11}(\mu_b+\phi)I_b \quad (3.16)$$

Hence $\dot{V} \leq 0$, if each of $(d_1-d_3),(d_2-d_1),(d_1-d_7),(d_1-d_2),(d_3-d_4),(d_7-d_1),(d_4-d_5),(d_4-d_7),(d_5-d_6),(d_6-d_7) \geq 0$.
Therefore, the largest compact invariant set in $(S_h,V_h,E_h,I_h,Q,T,R,S_b,V_b,E_b,I_b)\Omega$: $\dot{V}(S_h,V_h,E_h,I_h,Q,T,R,S_b,V_b,E_b,I_b) = 0$ is the singleton E^+, which E^+ is disease-free equilibrium. Therefore, every solution that starts in Ω approaches E^+ as $t \to \infty$: This shows that E^+ is globally asymptotically stable in Ω.

Global stability of endemic equilibrium of the model

Herein, we study the global behavior of the endemic equilibrium E^* for the model (2.1), in the sense of ([1, 5, 6, 10]).

Theorem 4. *If $R_0 > 1$, the unique endemic equilibrium E^* is globally asymptotically stable on Ω.*

Proof. Define $L:\{(S_h,V_h,E_h,I_h,Q,T,R,S_b,V_b,E_b,I_b) \in \Omega: S_h,V_h,E_h,I_h,Q,T,R,S_b,V_b,E_b,I_b > 0\} \to R$ by

$$L(t) = S_h^*\left(\frac{S_h}{S_h^*} - ln\frac{S_h}{S_h^*}\right) + V_h^*\left(\frac{V_h}{V_h^*} - ln\frac{V_h}{V_h^*}\right) + E_h^*\left(\frac{E_h}{E_h^*} - ln\frac{E_h}{E_h^*}\right) + P_1 I_h^*\left(\frac{I_h}{I_h^*} - ln\frac{I_h}{I_h^*}\right) + P_2 Q^*\left(\frac{Q}{Q^*} - ln\frac{Q}{Q^*}\right) + P_3 T^*\left(\frac{T}{T^*} - ln\frac{T}{T^*}\right) + P_4 R^*\left(\frac{R}{R^*} - ln\frac{R}{R^*}\right) + S_b^*\left(\frac{S_b}{s_b^*} - ln\frac{S_b}{S_b^*}\right) + V_b^*\left(\frac{V_b}{V_b^*} - ln\frac{V_b}{V_b^*}\right) + E_b^*\left(\frac{E_b}{E_b^*} - ln\frac{E_b}{E_b^*}\right) + P_5 I_b^*\left(\frac{I_b}{I_b^*} - ln\frac{I_b}{I_b^*}\right) \quad (3.17)$$

and the time derivative of L along the solutions of system of (2.1), is defined and continuous for all
$S_h,V_h,E_h,I_h,Q,T,R,S_b,V_b,E_b,I_b > 0$ and satisfies

$$\frac{dL}{dt} = \frac{\partial L}{\partial S_h}\frac{dS_h}{dt} + \frac{\partial L}{\partial V_h}\frac{dV_h}{dt} + \frac{\partial L}{\partial E_h}\frac{dE_h}{dt} + \frac{\partial L}{\partial I_h}\frac{dI_h}{dt} + \frac{\partial L}{\partial Q}\frac{dQ}{dt} + \frac{\partial L}{\partial T}\frac{dT}{dt} + \frac{\partial L}{\partial R}\frac{dR}{dt} + \frac{\partial L}{\partial S_b}\frac{dS_b}{dt} + \frac{\partial L}{\partial V_b}\frac{dV_b}{dt} + \frac{\partial L}{\partial E_b}\frac{dE_b}{dt} + \frac{\partial L}{\partial I_b}\frac{dI_b}{dt},$$

which becomes

Article DOI: 10.52589/AJMSS-KSUGFI1Z
DOI URL: https://doi.org/10.52589/AJMSS-KSUGFI1Z

African Journal of Mathematics and Statistics Studies
ISSN: 2689-5323
Volume 8, Issue 3, 2025 (pp. 136-161)
www.abjournals.org

$$\dot{L}(S_h, V_h, E_h, I_h, Q, T, R, S_b, V_b, E_b, I_b) = \left(1 - \frac{S_h^*}{S_h}\right)\dot{S}_h + \left(1 - \frac{V_h^*}{V_h}\right)\dot{V}_h + \left(1 - \frac{E_h^*}{E_h}\right)\dot{E}_h + P_1\left(1 - \frac{I_h^*}{I_h}\right)\dot{I}_h + P_2\left(1 - \frac{Q^*}{Q}\right)\dot{Q} + P_3\left(1 - \frac{T^*}{T}\right)\dot{T} + P_4\left(1 - \frac{R^*}{R}\right)\dot{R} + \left(1 - \frac{S_b^*}{S_b}\right)\dot{S}_b + \left(1 - \frac{V_b^*}{V_b}\right)\dot{V}_b + \left(1 - \frac{E_b^*}{E_b}\right)\dot{E}_b + P_5\left(1 - \frac{I_b^*}{I_b}\right)\dot{I}_b. \quad (3.18)$$

On substituting the derivative in (2.1) into (3.18),

$$\dot{L} = \left(1 - \frac{S_h^*}{S_h}\right)[\wedge_h - \beta S_h I_b - \beta_h S_h I_h - (\mu_h + \rho + \varepsilon)S_h + \alpha R + \psi_h V_h] + \left(1 - \frac{V_h^*}{V_h}\right)[\rho S_h - (\psi_h + \mu_h)V_h] + \left(1 - \frac{E_h^*}{E_h}\right)[\beta S_h I_b + \beta_h S_h I_h - (\mu_h + \sigma_h)E_h] + P_1\left(1 - \frac{I_h^*}{I_h}\right)[\sigma_h E_h - (k + \gamma_1 + \eta + \mu_h + \phi_h)I_h] + P_2\left(1 - \frac{Q^*}{Q}\right)[kI_h - (\delta + \mu_h + \phi)Q] + P_3\left(1 - \frac{T^*}{T}\right)[\eta I_h + \delta Q - (\mu_h + \gamma_2)T] + P_4\left(1 - \frac{R^*}{R}\right)[\gamma_2 T + \gamma_1 I_h + \varepsilon S_h - (\mu_h + \alpha)R] + \left(1 - \frac{S_b^*}{S_b}\right)[\wedge_b - \beta_b S_b I_b - (\mu_b + \rho_b)S_b + \psi_b V_b] + \left(1 - \frac{V_b^*}{V_b}\right)[\rho_b S_b - (\psi_b + \mu_b)V_b] + \left(1 - \frac{E_b^*}{E_b}\right)[\beta_b S_b I_b - (\sigma_b + \mu_b)E_b] + P_5\left(1 - \frac{I_b^*}{I_b}\right)[\sigma_b E_b - (\mu_b + \phi_b)I_b], \quad (3.19)$$

where

$$\wedge_h = \beta S_h^* I_b^* + \beta_h S_h^* I_h^* + (\mu_h + \rho + \varepsilon)S_h^* - \alpha R^* - \psi_h V_h^*,$$

$$\rho = (\psi_h + \mu_h)\frac{V_h^*}{S_h^*},$$

$$(\sigma_b + \mu_b) = \frac{\beta_b S_b^* I_b^*}{E_b^*},$$

$$\sigma_h = (k + \gamma_1 + \eta + \mu_h + \phi_h)\frac{I_h^*}{E_h^*},$$

$$(\mu_h + \sigma_h) = \frac{\beta S_h^* I_b^* + \beta_h S_h^* I_h^{**}}{E_h},$$

$$k = (\delta + \mu_h + \phi)\frac{Q^*}{I_h^*},$$

$$\wedge_b = \beta_b S_b^* I_b^* + (\mu_b + \rho_b)S_b^* - \psi_b V_b^*,$$

$$\sigma_b = \frac{(\mu_b + \phi_b)I_b^*}{E_b^*},$$

$$(\mu_h + \gamma_2) = \frac{\eta I_h^* + \delta Q^*}{T^*}, (\mu_h + \alpha) = \frac{[\gamma_2 T^* + \gamma_1 I_h^* + \varepsilon S_h^*]}{R^*}$$

and $\rho_b = \frac{(\psi_b + \mu_b)V_b^*}{S_b^*}$.

Substituting the values above into (3.19) and after simplification,

$$\dot{L} \leq -[\left(1 - \frac{S_h^*}{S_h}\right)[(\beta(S_h I_b - S_h^* I_b^*) + \beta_h(S_h I_h - S_h^* I_h^*) + (\mu_h + \rho + \varepsilon)(S_h - S_h^*) + \psi_h(V_h^* - V_h) + \alpha(R^* - R)] + (\psi_h + \mu_h)\left(1 - \frac{V_h^*}{V_h}\right)\left[\frac{(V_h S_h^* - V_h^* S_h)}{S_h^*}\right] + \left(1 - \frac{E_h^*}{E_h}\right)\left[\frac{\beta(S_h^* I_b^* E_h - S_h I_b E_h^*) + \beta_h(S_h^* I_h^* E_h - S_h I_h E_h^*)}{E_h^*}\right] + (k + \gamma_1 + \eta + \mu_h + \phi_h)P_1\left(1 - \frac{I_h^*}{I_h}\right)\left[\frac{(I_h E_h^* - I_h^* E_h)}{E_h^*}\right] + (\delta + \mu_h + \phi)P_2\left(1 - \frac{Q^*}{Q}\right)\left[\frac{(QI_h^* - Q^* I_h)}{I_h^*}\right] + P_3\left(1 - \frac{T^*}{T}\right)\left[\frac{(\eta I_h^* + \delta Q^*)T - (\eta I_h + \delta Q)T^*}{T^*}\right] + P_4\left(1 - \frac{R^*}{R}\right)\left[\frac{[\gamma_2 T^* + \gamma_1 I_h^* + \varepsilon S_h^*]R - [\gamma_2 T + \gamma_1 I_h + \varepsilon S_h]R^*}{R^*}\right] + \left(1 - \frac{S_b^*}{S_b}\right)[(\mu_b + \rho_b)(S_b - S_b^*) + \psi_b(V_b^* - V_b) +$$

Article DOI: 10.52589/AJMSS-KSUGFI1Z
DOI URL: https://doi.org/10.52589/AJMSS-KSUGFI1Z

African Journal of Mathematics and Statistics Studies
ISSN: 2689-5323
Volume 8, Issue 3, 2025 (pp. 136-161)
www.abjournals.org

$\beta_b(S_bI_b - S_b^*I_b^*)] + (\psi_b + \mu_b)\left(1 - \frac{V_b^*}{V_b}\right)\left[\frac{(V_bS_b^* - V_b^*S_b)}{S_b^*}\right] + \left(1 - \frac{E_b^*}{E_b}\right)\left[\frac{\beta_b(S_b^*I_b^*E_b - S_bI_bE_b^*)}{E_b^*}\right] +$
$P_5\left(1 - \frac{I_b^*}{I_b}\right)\left[\frac{(\mu_b+\phi_b)(I_bE_b^* - I_b^*E_b)}{E_b^*}\right]$]. (3.20)

Hence, $\dot{L} < 0$ if and only if $P_1, P_2, P_3, P_4, P_5 > 0$. Note that, $\dot{L} = 0$ if and only if $S_h = S_h^*$, $V_h = V_h^*$, $E_h = E_h^*$, $I_h = I_h^*$, $Q = Q^*$, $T = T^*$, $R = R^*$, $S_b = S_b^*$, $V_b = v_b^*$, $E_b = E_b^*$, and $I_b = I_b^*$. Therefore the largest compact invariant set in $\{(S_h, V_h, E_h, I_h, Q, T, R, S_b, V_b, E_b, I_b) \in \Omega : \dot{L} = 0\}$ is the singleton E^*, where E^* is the endemic equilibrium of the system (2.1), By LaSalle's invariance principle, it implies that E^* is globally asymptotically stable in the interior of Ω.

SENSITIVITY ANALYSIS AND NUMERICAL SIMULATION

Sensitivity Analysis of the Model

Preamble

Here we observe the changes happening in avian influenza infection transmission dynamics by computing the sensitivity indices of the reproductive number. Sensitivity analysis and simulations are important to discover how best we can minimize the effect of influenza, by studying the relative importance of different factors responsible for its transmission and prevalence with respect to the parameter values in the model. With the Sensitivity analysis we can determine the parameters which have high impact on reproductive number and can be used to estimate the relative change in the parameter with relative change in the reproductive number. The normalized forward sensitivity index of a variable to a parameter is the ratio of the relative change in the variable to the relative change in the parameter. Using the approach in [2, 13], we derived the analytical expression for sensitivity index of $R_0^{b,h}$ to each parameter. The parameter values used in this section are shown in Table 1 , chosen from the realistic ranges for illustrative purpose.

Sensitivity indices of $R_0^{b,h}$

Since we have the explicit expressions for $R_0^{b,h}$, we can derive an analytical expression for its sensitivity to each parameter using the normalized forward sensitivity index as described below

Definition 2. *The normalized forward sensitivity index of a variable Q that depends, differentially, on a parameter m , is defined as:* $Z_m^Q = \frac{\partial Q}{\partial m} \times \frac{m}{Q}$

We derive the sensitivity indices of various reproductive numbers $R_0^{b,h}$ corresponding to the following parameters: Λ_h, Λ_b, β_h, β_b, ε, σ_h, σ_b, γ_1, ϕ_h, ϕ_b, μ_h, μ_b, α, η, ρ, ρ_b, ψ_h, ψ_b, k as follows, for example:

$$for\ example, \quad Z_m^{R_0} = \frac{\partial R_0}{\partial m} \times \frac{m}{R_0}$$

Therefore, the sensitivity index of $R_0^{b,h}$ with respect to Λ_h, Λ_b, β_h and β_b are obtained using the data in Table 1, as follows:

Article DOI: 10.52589/AJMSS-KSUGFI1Z
DOI URL: https://doi.org/10.52589/AJMSS-KSUGFI1Z

African Journal of Mathematics and Statistics Studies
ISSN: 2689-5323
Volume 8, Issue 3, 2025 (pp. 136-161)
www.abjournals.org

$$Z_{\Lambda_h}^{R_0^{b,h}} = \frac{\partial R_0^{b,h}}{\partial \Lambda_h} \times \frac{\Lambda_h}{R_0^{b,h}} = +1.00000\ Z_{\Lambda_b}^{R_0^{b,h}} = \frac{\partial R_0^{b,h}}{\partial \Lambda_b} \times \frac{\Lambda_b}{R_0^{b,h}} = +1.00000\ Z_{\beta_h}^{R_0^{b,h}} = \frac{\partial R_0^{b,h}}{\partial \beta_h} \times \frac{\beta_h}{R_0^{b,h}}$$
$$= +1.00000\ Z_{\beta_b}^{R_0^{b,h}} = \frac{\partial R_0^{b,h}}{\partial \beta_b} \times \frac{\beta_b}{R_0^{b,h}} = +1.00000\ Z_{\varepsilon}^{R_0^{b,h}} = \frac{\partial R_0^{b,h}}{\partial \varepsilon} \times \frac{\varepsilon}{R_0^{b,h}}$$
$$= -0.19196\ \}$$

The remaining indices are generated via the same method and presented in Table 3 The sensitivity results of the model parameters of $R_0^{b,h}$ is given in Table 3 and the graphical illustration is given in Figure 2.

Table 2: Parameter values of avian influenza model

Symbol	Estimated value	Reference	Symbol	Estimated value	Reference
Λ_h	1000	Assumed	ϕ	0.01	Assumed
Λ_b	30	Assumed	μ_h	0.033	Assumed
β_h	0.1025	[30]	μ_b	0.333	Assumed
β_b	0.012	[27]	α	0.699	[26]
β	0.2	[21]	ρ	[0 - 1.0]	Assumed
ε	[0 - 1.0]	Assumed	ρ_b	[0 - 1.0]	Assumed
σ_h	0.05	Assumed	ψ_h	0.002	Assumed
σ_b	0.85	Assumed	ψ_b	0.003	Assumed
γ_1	0.3	Assumed	k	[0 - 1.0]	Assumed
γ_2	0.7	[17, 30]	η	[0 - 1.0]	Assumed
ϕ_h	0.03	[26]	δ	0.6	Assumed
ϕ_b	0.75	[3]			

Table 3: Sensitivity indices for $R_0^{b,h}$

Parameters Value	Sensitivity indices to $R_0^{b,h}$	Parameters Value	Sensitivity indices to $R_0^{b,h}$
Λ_h	1.000000000	μ_h	-0.5207168550
Λ_b	1.000000000	μ_b	-0.2422008282
β_h	1.000000000	α	0.1411460687
β_b	1.000000000	η	-0.4265402843
ε	-0.1919606864	ρ	-0.7769608783
σ_h	0.2857142853	ρ_b	-0.9471585237
σ_b	1.000000001	ψ_h	0.06249999995
γ_1	-0.2369668246	ψ_b	0.05361274665
ϕ_h	-0.03791469194	k	-0.2843601895
ϕ_b	-0.9230769225		

Article DOI: 10.52589/AJMSS-KSUGFI1Z
DOI URL: https://doi.org/10.52589/AJMSS-KSUGFI1Z

African Journal of Mathematics and Statistics Studies
ISSN: 2689-5323
Volume 8, Issue 3, 2025 (pp. 136-161)
www.abjournals.org

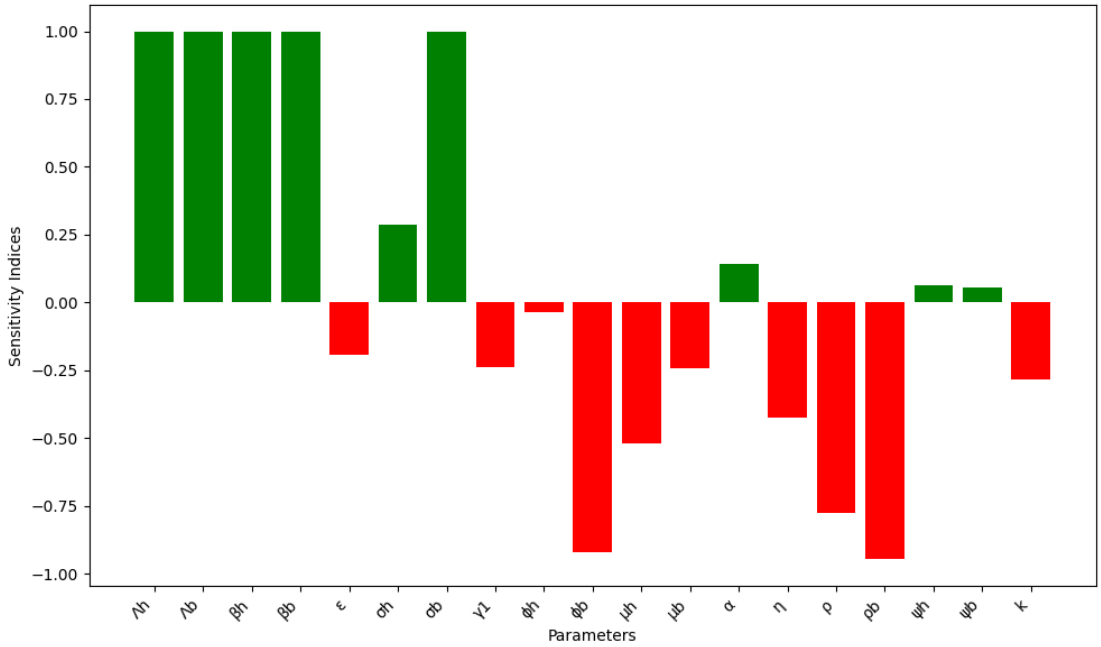

Figure 2: Plot showing the sensitivity indices of the model reproductive ratio with respect to parameters

Table 3 shows the sensitivity indices of R_0 with respect to each of the nineteen parameters involved. The highly sensitive parameters to the reproductive number include, $\rho_b, \phi_b, \rho, \mu_h, \eta, k, \mu_b, \gamma_1, \varepsilon, \phi_h$, while the minimum sensitive parameter, which is the contact rate β_h, β_b and the recruitment rate for both humans and birds Λ_h,Λ_b, followed by $\sigma_b, \sigma_h, \alpha, \psi_h, \psi_b$. From Table 3, the indices with positive signs show that the value of $R_0^{b,h}$ increases when the corresponding parameters are increased and indices with negative signs indicate that the value of $R_0^{b,h}$ decreases with an increase in the corresponding parameters. This analysis is done to ascertain which parameters dominate the results of our analysis. Therefore, it is clear from Table 3 above that it $R_0^{b,h}$ will decrease with increases in the values of the relevant parameters, since the sensitivity indices of these parameters are negative.

Numerical Simulation and Remark

Numerical simulation

The numerical simulation was conducted for the model via the fourth-order Runge-Kutta scheme in Maple and Matlab programming software. The aim of the exercise is to validate numerically the analytic results earlier obtained for model (2.1). For each simulation phase, the corresponding parameter value(s) indicated in Table 1 is/are employed with the initial state variables chosen as, $S_h(0) = 2548$, $V_h(0) = 20$, $E_h(0) = 400$, $I_h(0) = 10$, $Q(0) = 6$, $T(0) = 6$, $R(0) = 10$, $S_b(0) = 335$, $V_b(0) = 50$, $E_b(0) = 100$ and $I_b(0) = 15$. The vaccination rates (ρ_b, ρ), quarantine rate (k), treatment rate (η) and immunity gain (ε) are used to compute the value of $R_0^{b,h}$, and the numerical results are presented in Tables 4 - 8 . In addition, the simulation graphs are drawn for various values of the key parameters and presented in Figures 5 to 8.

Article DOI: 10.52589/AJMSS-KSUGFI1Z
DOI URL: https://doi.org/10.52589/AJMSS-KSUGFI1Z

African Journal of Mathematics and Statistics Studies
ISSN: 2689-5323
Volume 8, Issue 3, 2025 (pp. 136-161)

www.abjournals.org

Table 4: Effect of varying the parameters ρ against ρ_b, k, η, ε on $R_0^{b,h}$

ρ	ρ_b	k	η	ε	$R_0^{b,h}$
0.0	0.95	0.9	0.9	0.7	7.59
0.2	0.95	0.9	0.9	0.7	1.93
0.4	0.95	0.9	0.9	0.7	1.11
0.6	0.95	0.9	0.9	0.7	0.78
0.8	0.95	0.9	0.9	0.7	0.60
1.0	0.95	0.9	0.9	0.7	0.49

Table 5: Effect of varying the parameters ρ_b against ρ, k, η, ε on $R_0^{b,h}$

ρ_b	ρ	k	η	ε	$R_0^{b,h}$
0.0	0.8	0.9	0.9	0.7	2.29
0.2	0.8	0.9	0.9	0.7	1.43
0.4	0.8	0.9	0.9	0.7	1.04
0.6	0.8	0.9	0.9	0.7	0.82
0.8	0.8	0.9	0.9	0.7	0.68
1.0	0.8	0.9	0.9	0.7	0.58

Table 6: Effect of varying the parameters k against ρ_b, ρ, η, ε on $R_0^{b,h}$

k	ρ_b	ρ	η	ε	$R_0^{b,h}$
0.0	0.8	0.6	0.9	0.7	1.42
0.2	0.8	0.6	0.9	0.7	1.25
0.4	0.8	0.6	0.9	0.7	1.12
0.6	0.8	0.6	0.9	0.7	1.01
0.8	0.8	0.6	0.9	0.7	0.92
1.0	0.8	0.6	0.9	0.7	0.84

Table 7: Effect of varying the parameters η against ρ_b, ρ, k, ε on $R_0^{b,h}$

η	ρ_b	ρ	k	ε	$R_0^{b,h}$
0.0	0.75	0.7	0.9	0.7	1.29
0.2	0.75	0.7	0.9	0.7	1.14
0.4	0.75	0.7	0.9	0.7	1.02
0.6	0.75	0.7	0.8	0.7	0.92
0.8	0.75	0.7	0.9	0.7	0.84
1.0	0.75	0.7	0.9	0.7	0.77

Article DOI: 10.52589/AJMSS-KSUGFI1Z
DOI URL: https://doi.org/10.52589/AJMSS-KSUGFI1Z

African Journal of Mathematics and Statistics Studies
ISSN: 2689-5323
Volume 8, Issue 3, 2025 (pp. 136-161)
www.abjournals.org

Table 8: Effect of varying the parameters ε against ρ_b, ρ, k, η on $R_0^{b,h}$

ε	ρ_b	ρ	k	η	$R_0^{b,h}$
0.0	0.8	0.6	0.85	0.7	1.04
0.2	0.8	0.6	0.85	0.7	1.02
0.4	0.8	0.6	0.85	0.7	1.01
0.6	0.8	0.6	0.85	0.7	0.99
0.8	0.8	0.6	0.85	0.7	0.98
1.0	0.8	0.6	0.85	0.7	0.96

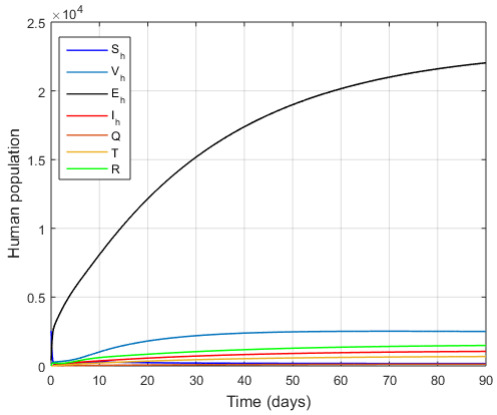

Figure 3: Plot showing behaviour of the of the human state variables

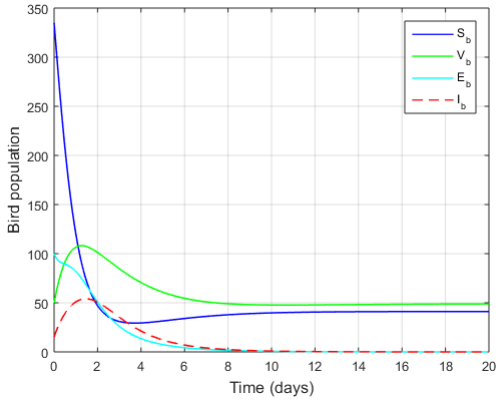

Figure 4: Plot showing behaviour bird state variables

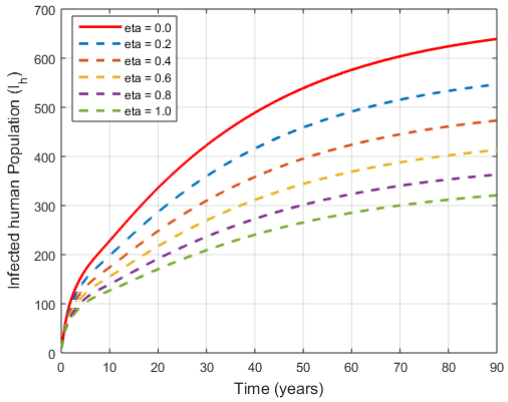

Figure 5: Graphs showing the effect of varying varying values of η on infected humans

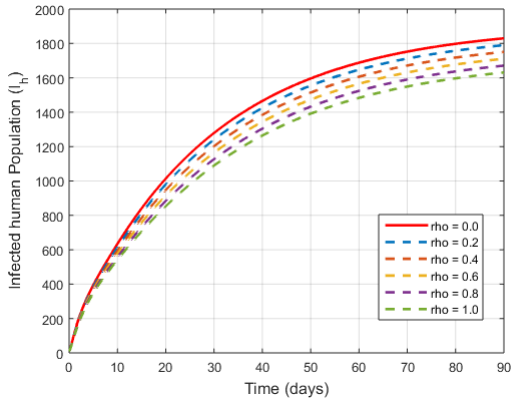

Figure 6: Graphs showing the effect of values of ρ on infected humans.

Article DOI: 10.52589/AJMSS-KSUGFI1Z
DOI URL: https://doi.org/10.52589/AJMSS-KSUGFI1Z

African Journal of Mathematics and Statistics Studies
ISSN: 2689-5323
Volume 8, Issue 3, 2025 (pp. 136-161)
www.abjournals.org

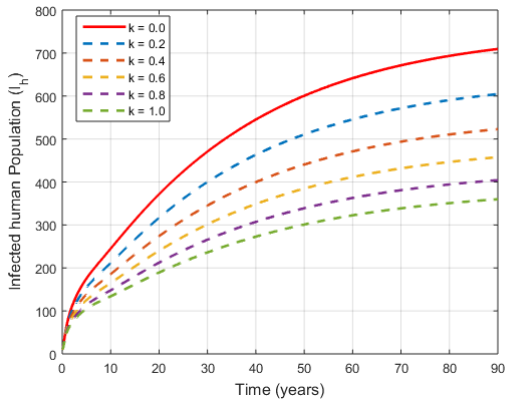

Figure 7: Graphs showing the effect of varying of values of k on infected humans

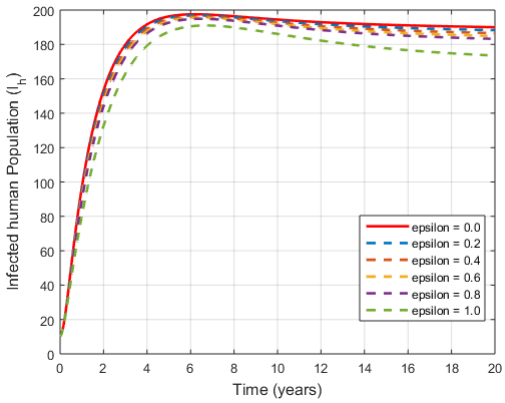

Figure 8: Graphs showing the effect varying values of ε on infected humans

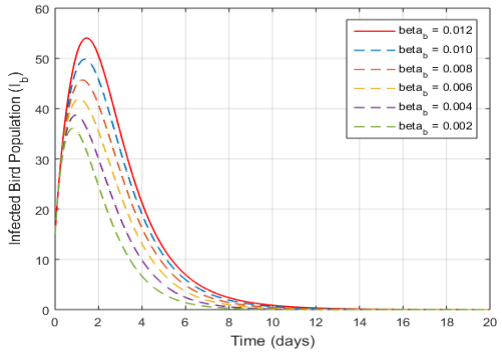

Figure 9: Graph of infected bird with varying human bird-to-bird contact rate β_b

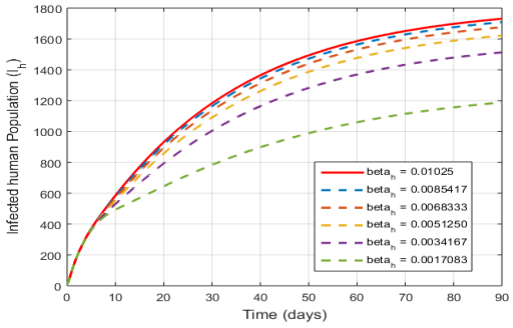

Figure 10: Graph displaying the infected with varying human-to-human contact rate β_h

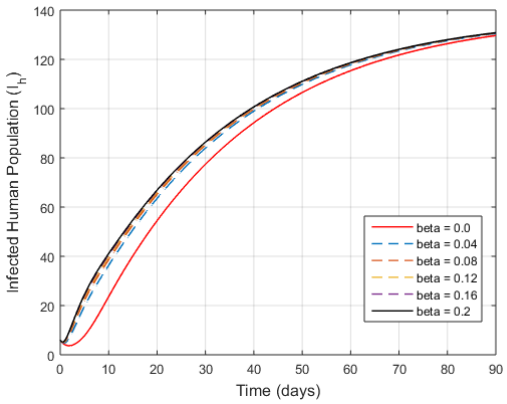

Figure 11: Graph displaying the infected human with varying bird-to-human contact rate β

Article DOI: 10.52589/AJMSS-KSUGFI1Z
DOI URL: https://doi.org/10.52589/AJMSS-KSUGFI1Z

African Journal of Mathematics and Statistics Studies
ISSN: 2689-5323
Volume 8, Issue 3, 2025 (pp. 136-161)
www.abjournals.org

Remarks on results from numerical simulation

Table 4 demonstrates that the vaccination rate significantly impacts the reproductive ratio. Specifically, $R_0^{b,h} > 1$ when the human population is not vaccinated against avian influenza ($\rho = 0\%$), indicating that the disease can spread in an unvaccinated population. However, when at least 60% of the human population is vaccinated, $R_0^{b,h} < 1$, signifying that vaccination effectively reduces the transmission potential, ultimately leading to disease control or eradication. Table 5 illustrates that vaccinating at least 60% of the bird population against avian influenza, with parameters $\rho = 80\%$, $k = 90\%$, $\eta = 90\%$, and $\varepsilon = 70\%$, results in $R_0^{b,h} < 1$. This indicates that under these vaccination conditions, the spread of avian influenza can be effectively controlled within both bird and human populations, reducing the potential for an outbreak.

Table 6 demonstrates that if at least 80% of infected humans with avian influenza are quarantined, along with vaccination rates of $\rho_b = 80\%$ in birds and $\rho = 60\%$ in humans, and parameters $\eta = 90\%$ and the reproductive ratio $R_0^{b,h} < 1$. This indicates that effective quarantine measures, combined with vaccination efforts, can significantly reduce the spread of avian influenza, controlling the infection within both bird and human populations. Table 7 shows that when at least 60% of infected humans with avian influenza receive treatment, combined with vaccination rates of $\rho_b = 60\%$ in birds, $\rho = 70\%$ in humans, and parameters immunity gain $\varepsilon = 70\%$, the reproductive ratio $R_0^{b,h} < 1$. This indicates that an effective treatment strategy, alongside vaccination, plays a crucial role in controlling the spread of avian influenza and reducing the risk of an outbreak.

Table 8 indicates that at the initial stage, when human immunity is 0%, $R_0^{b,h} > 1$, meaning the disease can spread widely. However, when at least 60% of the human population possesses immunity at the initial stage ($\varepsilon = 60\%$), along with vaccination rates of $\rho_b = 80\%$ in birds, $\rho = 60\%$ in humans, and parameters $k = 85\%$ and $\eta = 80\%$, the reproductive ratio $R_0^{b,h} < 1$. This demonstrates that achieving a sufficient level of initial immunity in humans, together with vaccination, significantly reduces the transmission of avian influenza, preventing an outbreak. Therefore, it is evident from Tables 4 to 8 that the reproductive ratio $R_0^{b,h}$ decreases as the rates of vaccination, quarantine, treatment, and initial immunity increase. This highlights the critical role these interventions play in reducing the spread of avian influenza across both human and bird populations.

Figure 5 demonstrates that increasing vaccination coverage (ρ) significantly reduces the infected human population over time. Figure 6 demonstrates how different treatment rates (η) impact the infected human population (I_h) over time. As the treatment rate increases from 0 to 1.0, the number of infected individuals decreases significantly. Without treatment ($\eta = 0$), the infected population grows rapidly and stabilizes at a high level (approximately 650). As treatment rates increase, the infection spreads more slowly, and the total number of infected individuals drops, with the highest treatment rate ($\eta = 1.0$), keeping the infected population below 200. This highlights the importance of treatment in controlling avian influenza infections, showing that higher treatment rates lead to a substantial reduction in the infected population over time, preventing large-scale outbreaks.
The graph in Figure 7 illustrates the impact of quarantine (k) on the infected human population (I_h) over time. When no quarantine is implemented ($k = 0$), the infected population grows

Article DOI: 10.52589/AJMSS-KSUGFI1Z
DOI URL: https://doi.org/10.52589/AJMSS-KSUGFI1Z

African Journal of Mathematics and Statistics Studies
ISSN: 2689-5323
Volume 8, Issue 3, 2025 (pp. 136-161)
www.abjournals.org

rapidly, stabilizing at a high level (approximately 700) over time. As quarantine measures are gradually introduced, with k increasing from 0 to 1.0, the infected population drops drastically. At the highest quarantine level ($k = 1.0$), the infected population is significantly reduced, stabilizing below 400. This sharp decline demonstrates that quarantine is highly effective in controlling the spread of infection by isolating individuals and preventing further transmission. Figure 8 illustrates that increasing the initial immunity level in the population reduces both the peak and the long-term number of infected individuals. Hence, in Figures 4 to 11, it was found that an increase in immunity at the initial stage, through vaccination of both birds and humans, and treatment provided to humans, results in a lower infection rate in both bird and human populations. Similarly, a higher contact rate, whether from bird to bird, bird to human, or human to human (β, β_b, β_h) correlates with an increased rate of infection.

CONCLUSION

In this work, a deterministic bird-human avian influenza model for an open population is formulated and analyzed for the dynamics of avian influenza transmission from birds to humans. The model includes vaccination, quarantine, and treatment as strategies to reduce infection. In addition, the model incorporates the recruitment of new individuals into the susceptible class through birth or immigration, with the possibility that immigrant individuals exposed to the disease can also enter the susceptible class. Prevention strategies, including vaccination, quarantine, and treatment, are integrated into the model to assess their potential impact on the transmission dynamics of the disease. The positivity of the solutions to the state variables in the model equations has been affirmed, indicating that the deterministic model aligns with reality. The model equilibria are discussed along with their stability properties. Formulae for computing the basic reproductive ratio ($R_0^{b,h}$) have been derived. Another analytical result obtained in this study is that the model is asymptotically stable when the trace of the Jacobian matrix obtained for the state equations is negative and its determinant is positive. This is implying $R_0^{b,h} < 1$. In conducting a sensitivity analysis of the model, the normalized sensitivity indices of $R_0^{b,h}$ show that the most sensitive parameters are with a negative sign, which shows that increasing the rate of controlling infected individuals reduces the value, $R_0^{b,h}$ while the least sensitive parameters are with a positive sign, which indicates that reducing the contact rate of exposed individuals reduces the value of $R_0^{b,h}$. Numerical simulations are conducted with the model, and it is found that the infection will be reduced and the disease will die out if the rate of vaccination, quarantine and treatment is high. Likewise, if individuals possess strong immunity at the initial stage, then the disease will be minimized in the populace.

The results obtained are graphically illustrated for a better understanding of the scenarios through MATLAB computer programming. The results suggest that increasing the effort on the following control parameters—vaccination rates (ρ, ρ_b), quarantine rate (k), treatment rate (η), immunity gain at the initial stage (ε), and effective contact rates (β_b, β_h, β) is more effective in reducing avian influenza disease in society.

Article DOI: 10.52589/AJMSS-KSUGFI1Z
DOI URL: https://doi.org/10.52589/AJMSS-KSUGFI1Z

REFERENCES

[1] Adda, P., and Bichara, D. (2011). Global stability for SIR and SIRS models with differential mortality. *Equipe-projet Masaie et Universite de Metz LMAM (UMR CNRS 7122) ISGMP*, 8(8), 1–17.
[2] Adeosun, M. E., Akin-Awoniran, B. O., and Akingbade, J. A. (2022). A novel mathematical model for curbing the spread of Covid-19 in Nigeria. *International Journal of Mathematics Trends and Technology*, 68.
[3] Agusto, F. B., and Gumel, A. B. (2010). Theoretical assessment of avian influenza vaccine. *DCDS Series B*, 13(1), 1–25.
[4] Ainea, N., Massawe, E. S., Makinde, O. D., and Namkinga, L. (2015). Mathematical analysis of control strategies of HCV in a community with an inflow of infected immigrants. *Advances in Infectious Diseases*, 5(1), 1.
[5] Akingbade, J. A., Adetona, R. A., and Ogundare, B. S. (2018). Mathematical model for the study of transmission and control of measles with immunity at the initial stage. *Malaya Journal of Matematik*, 6(4), 823–834.
[6] Akingbade, J. A., and Ogundare, B. S. (2021). Boundedness and stability properties of solutions of mathematical model of measles. *Tamkang Journal of Mathematics*, 52(1), 91–112.
[7] Alexakis, L., Buczkowski, H., Ducatez, M., Fusaro, A., Gonzales, J. L., Kuiken, T., and Kohnle, L. (2025). Avian influenza overview September–December 2024. *EFSA Journal*, 23(1), e9204.
[8] Alexander, M. E., Bowman, C., Moghadas, S. M., Summers, R., Gumel, A. B., and Sahai, B. M. (2004). A vaccination model for transmission dynamics of influenza. *SIAM J. Appl. Dyn. Syst.*, 3(4), 503–524.
[9] Awasthi, A. K., Kumar, S., and Garov, A. K. (2021). A mathematical model for stability analysis of COVID-like epidemic/endemic/pandemic. *medRxiv*.
[10] Bame, N., Bowong, S., Mbang, J., Sallet, G., and Tewa, J. J. (2008). Global stability analysis for SEIS models with n latent classes. *Mathematical Biosciences and Engineering*, 5(1), 20.
[11] Centres for Disease Control and Prevention. (2005). Key facts about avian influenza (bird flu) and avian influenza A (H5N1) virus. Available at: https://www.cdc.gov/flu/avian/gen-info/facts.htm.
[12] Centres for Disease Control and Prevention. (2012). National Centre for immunization and respiratory diseases (NCIRD): Influenza vaccination coverage. Available at: https://www.cdc.gov/flu/fluvaxview/trends/adults-over18.htm.
[13] Chitnis, N., Hyman, J. M., and Cushing, J. M. (2008). Determining important parameters in the spread of malaria through the sensitivity analysis of a mathematical model. *Bulletin of Mathematical Biology*, 70(5), 1272.
[14] David, J. D., Earn, J. D., and Simon, A. L. (2002). Ecology and evolution of the flu. *Trends in Ecology & Evolution*, 17(7).
[15] Diekmann, O., and Heesterbeek, J. A. P. (2000). *Mathematical Epidemiology of Infectious Diseases: Model Building, Analysis and Interpretation*. John Wiley & Sons.
[16] Evirgen, F., Uçar, E., Uçar, S., and Ozdemir, N. (2023). Modelling influenza A disease dynamics under Caputo-Fabrizio fractional derivative with distinct contact rates. *Mathematical Modelling and Numerical Simulation with Applications*, 3(1), 58–73.
[17] Galvin, C. J., Rumbos, A., Vincent, J. I., and Salvato, M. (2014). Modeling the effects of avian flu (H5N1) vaccination strategies on poultry. CODEE Journal, 10(1). Available at: https://scholarship.claremont.edu/codee/vol10/iss1/1.

Article DOI: 10.52589/AJMSS-KSUGFI1Z
DOI URL: https://doi.org/10.52589/AJMSS-KSUGFI1Z

[18] Gubar, E., and Zhu, Q. (2013). Optimal control of influenza epidemic model with virus mutations. In *2013 European Control Conference (ECC)*, 3125–3130. IEEE.
[19] Hayama, Y., Sawai, K., Yoshinori, M., Yamaguchi, E., and Yamamoto, T. (2022). Estimation of introduction time window of highly pathogenic avian influenza virus into broiler chicken farms during the 2020–2021 winter season outbreak in Japan. Preventive Veterinary Medicine, 208, 105768.
[20] Imran, M., Ben-Romdhane, M., Ansari, A. R., and Temimi, H. (2020). Numerical study of an influenza epidemic dynamical model with diffusion. Discrete & Continuous Dynamical Systems – S.
[21] Iwami, S., Takeuchi, Y., and Liu, X. (2007). Avian-human influenza epidemic model. *Mathematical Biosciences*, 207, 1–25.
[22] Kermack, W. O., and McKendrick, A. G. (1927). A contribution to the mathematical theory of epidemics. *Proceedings of the Royal Society of London A*, 115(772), 700–721.
[23] La Salle, J. P. (1976). *The Stability of Dynamical Systems*. Society for Industrial and Applied Mathematics.
[24] Mardlijah, M., Ariani, T. D., and Asfihani, T. (2017). Isolation strategy of a two-strain avian influenza model using optimal control. In *AIP Conference Proceedings* (Vol. 1867, No. 1). AIP Publishing.
[25] Mishra, B. K., and Sinha, D. N. (2016). A mathematical model on avian influenza with quarantine and vaccination. *Journal of Immunology and Infectious Diseases*, 4(2).
[26] Modnak, C. (2017). Mathematical modelling of an avian influenza: optimal control study for intervention strategies. *Applied Mathematics and Information Sciences*, 11(4), 1049–1057.
[27] Mohamed, D., and Abdesslam, B. (2008). An avian influenza mathematical model. *Applied Mathematical Sciences*, 2(36), 1749–1760.
[28] Putri, A. R., and Syafwan, M. (2020). Analytical study and numerical solutions of bird flu epidemic model with vaccination.
[29] Sangotola, A. O., and Onifade, A. A. (2019). A generalized SEIR mathematical model with infectivity in exposed period. *Journal of the Nigerian Mathematical Society*, 38(1), 45–54.
[30] Tchuenche, J. M., Khamis, S. A., Agusto, F. B., and Mpeshe, S. C. (2011). Optimal control and sensitivity analysis of an influenza model with treatment and vaccination. *Acta Biotheoretica*, 59(1), 1–28.
[31] Van den Driessche, P., and Watmough, J. (2002). Reproduction numbers and sub-threshold endemic equilibria for compartmental models of disease transmission. *Mathematical Biosciences*, 180(1–2), 29–48.
[32] Vargas-De-León, C. (2009). Constructions of Lyapunov functions for classic SIS, SIR and SIRS
epidemic models with variable population size. *Foro-RedMat: Revista Electrónica de Contenido Matemático*, 26, 1–12.
[33] Victor, A. O., and Oduwole, H. K. (2020). Stability analysis of disease-free equilibrium state for an endemic deterministic model for HIV/AIDS. *medRxiv*.
[34] Zheng, T., Nie, L., Zhu, H., Luo, Y., and Teng, Z. (2022). Role of seasonality and spatial heterogeneity in the transmission dynamics of avian influenza. *Nonlinear Analysis: Real World Applications*, 67, 103567.

Article DOI: 10.52589/AJMSS-KSUGFI1Z
DOI URL: https://doi.org/10.52589/AJMSS-KSUGFI1Z